The Utility of MRI for Measuring Hematocrit in Fetal Anemia

by

Jiawei Xu

A thesis submitted in conformity with the requirements
for the degree of Master of Science

Department of Physiology
University of Toronto

The Utility of MRI for Measuring Hematocrit in Fetal Anemia

Jiawei Xu

Master of Science

Department of Physiology
University of Toronto

2019

Abstract

Doppler ultrasound measurements of the peak systolic velocity of the middle cerebral artery (MCA) can be used to non-invasively diagnose fetal anemia but are less precise following fetal blood transfusion and in late gestation. We have previously demonstrated the feasibility of estimating fetal hematocrit *in vitro* using MRI relaxation times. The objective of this thesis is to report the use of MRI as a non-invasive tool to accurately detect fetal anemia *in vivo*. MRI-estimated hematocrit of the umbilical vein of fetuses undergoing fetal blood sampling or transfusion was compared against MCA Doppler and fetal blood sampling measurements. Excellent correlation and low systematic bias were found between MRI and laboratory measurements. MRI had higher specificity than MCA Doppler for detecting fetal anemia. Our results suggest there may be a role for fetal MRI as an adjunct to ultrasound in fetuses with suspected anemia, particularly following previous transfusion and in late gestation.

Acknowledgments

First and foremost, I would like to express my gratitude towards my supervisor, Dr. Mike Seed, for your trust, guidance and support over the past two years. Your vast knowledge, passion and kindness motivate me to push myself to be a better scientist and individual. It has been a pleasure working with you.

I am extremely grateful to my supervisory committee, Dr. Christopher Macgowan, Dr. Brian McCrindle, and Dr. John Kingdom for their insightful advice and for challenging my thinking. I would also like to thank the amazing CDIU staff at the Hospital for Sick Children, including Navjot Gill, Vivian Tassos, and Kelly Paredes for their help in organizing and performing the MRI scans. Special thanks to Dr. Sharon Portnoy for helping me with all my MRI questions and problems, and also for your input on the MRI section of this thesis.

A sincere thank you to everyone at Mount Sinai Hospital who contributed to this work: Dr. Johannes Keunan, Dr. Greg Ryan, Dr. Tim Van Mieghem, all the nurses at the Fetal-Maternal unit (Colleen, Bita, Leslie, Katie, Ingrid, Mary, Nancy and Moira), Natasha Milligan, Nancy Moniz, Michelle Rodrigues and all of the participants of the study. Without you, this study would not have been possible.

Thank you to the lovely former and current lab members: Jessie Mei Lim, Brahmdeep Saini, Amandeep Saini, Davide Marini, An Qi Duan, Tanroop Aujla, Kyung Sik Cho, Jiaqi Ren and Liqun Sun, for your patience in guiding me step by step throughout my study, for enduring my endless questions, for being a colleague, a friend and a family to me. I will forever remember the late nights we spent together editing essays, the random debates and discussions at lunch time and all the joy and laughter we shared. Special thanks to Jessie Mei, for being the best and cutest roommate ever!

I am grateful for the funding from Queen Elizabeth II and SGS scholarship at University of Toronto, and the Physicians' Services Incorporated Foundation for funding the study.

For the most important friends I have outside of the lab, Chuxi Pan, Haoyu Wan and Calvin Won, thank you for listening to me, offering me advice, helping me destress and encouraging me when I am down.

Finally, special thanks to my parents and my dear sister, Michelle, for always being there with your unconditional support and love through the good and bad times. Most importantly, thank you, sister, for feeding me when I was writing my thesis. You are the best gift to my life!

Contributions

The research presented in this thesis was adapted from the article Xu J, Duan AQ, Marini D, *et al*. "The utility of MRI for measuring hematocrit in fetal anemia". Am J Obstet Gynecol 2019 (In press). doi: 10.1016/j.ajog.2019.07.016.

The role of the author, **Jiawei Xu**, in this study includes participant recruitment, participation in the magnetic resonance imaging (MRI) scans, post-processing of the MRI images, data collection and analysis. The data used in this thesis included both participants recruited prior to and during the author's involvement in the study. The author was responsible of the writing of this thesis with the guidance and expertise of the following individuals:

Dr. Mike Seed conceived the study design, performed the MRI scans on the fetal subjects, provided guidance on the data analysis and interpretation, and also provided detailed revision of the thesis.

Dr. Davide Marini, **Ms. Navjot Gill**, and **Ms. Vivian Tassos** performed the MRI scans on the fetal subjects.

Ms. An Qi Duan contributed to the recruitment of participants and data collection prior to the author's involvement in the study.

Dr. John G. Sled provided guidance on the development of the MRI protocol.

Dr. Christopher K. Macgowan and **Dr. Sharon Portnoy** provided guidance on the development of the MRI protocol and the relaxometry, and also provided important feedback on the thesis.

Ms. Jessie Mei Lim performed the interobserver measurements for T_1 and T_2.

Dr. Brian McCrindle provided guidance on the statistically analyses and analysis approach and provided important feedback on the thesis.

Dr. John C. Kingdom and Dr. Johannes Keunen provided patients to recruit for the study from their clinics and their clinical expertise in fetal anemia and fetal therapy.

Table of Contents

List of Tables

List of Figures

List of Abbreviations

cffDNA	Cell free fetal DNA
FOV	Field of View
Hb	Hemoglobin
Hb_A	Adult hemoglobin
Hb_F	Fetal hemoglobin
Hct	Hematocrit
IPT	Intraperitoneal blood transfusion
IUT	Intrauterine blood transfusion
IVIG	Intravascular immunoglobin
IVT	Intravascular blood transfusion
MCA	Middle cerebral artery
MCA-PSV	Middle cerebral artery peak systolic velocity
MCDA	Monochorionic diamniotic
MRI	Magnetic resonance imaging
NDI	Neurodevelopmental impairment
RBC	Red blood cell
RF	Radiofrequency
SaO_2/sO_2	Oxygen saturation
SSFP	Steady-state Free Precession

T	Tesla
TAPS	Twin anemia polycythemia sequence
TE	Echo Time
TF	Repetition Time
TI	Inversion time
TTTS	Twin-to-twin transfusion

List of Appendices

1 Introduction

Fetal anemia is an uncommon pregnancy complication characterized by a low hematocrit or hemoglobin level. When moderate-to-severe, it may result in widespread tissue hypoxia, leading to hydrops fetalis and ultimately fetal demise.[1] Red blood cell alloimmunization is the most common cause of fetal anemia.[2] Commonly reported non-immune causes include alpha-thalassemia and parvovirus infection. The modern treatment for severe fetal anemia – ultrasound-guided intrauterine blood transfusion (IUT) - is associated with a survival rate of over 90% in non-hydropic fetuses.[3] While only 10% of affected pregnancies requires transfusion, the remaining 90% with less severe anemia will require regular monitoring. Follow-up post-transfusion is also crucial for determining the timing of subsequent transfusions, as fetal anemia usually recurs. Fetal blood sampling is the gold-standard diagnostic test for fetal anemia but is associated with risks of significant complications, including a fetal loss rate of 1-2%.[4] The measurement of peak systolic velocity in the middle cerebral artery (MCA-PSV) measured by Doppler ultrasound has proven to be a reliable screening test for fetal anemia.[3] However, recent studies have shown that MCA-PSV Doppler becomes less accurate after blood transfusions and in later gestations, thus highlighting the need for a complimentary diagnostic tool for fetal anemia.[5–9]

This first chapter is divided into two parts. A general overview of fetal anemia will be presented in Section 1.1, including the definition, pathophysiology (Section 1.1.1) and common causes of fetal anemia (Section 1.1.2). This is followed by an account of the diagnosis, treatment and management of affected pregnancies (Section 1.1.3). In the second part, the main methodology used in this study – magnetic resonance imaging (MRI) – will be described (Section 1.2). This section will start with an introduction of the basic physics theory behind MRI relaxometry (Section 1.2.1 and 1.2.2), characterize the relationship between MRI relaxation times and blood properties (Section 1.2.3), and finally describe how hematocrit can be estimated non-invasively using MRI relaxometry (Section 1.2.4).

1.1 Fetal Anemia

1.1.1 General Introduction

According to the Society of Maternal-Fetal Medicine Clinical Guidelines, fetal anemia can be defined as "a hemoglobin value of more than 2 SD below the mean".[2] Fetal hemoglobin and hematocrit levels are not constant over the course of pregnancy. Hemoglobin concentration increases from 14 g/dl at 22 weeks of gestation to 17 g/dL at 40 weeks, while hematocrit similarly increases from 40% to 53%.[10] To account for this change in hemoglobin, reference ranges are expressed either as deviation from the mean or as multiples of the median for gestational age (Table 1).[11] These criteria are relatively arbitrary with the intention to identify fetal anemia before the development of hydrops. In clinical care, a hematocrit level of < 30% is also used as an indicator of the presence of fetal anemia.[2]

Fetal animal and human studies have investigated the hemodynamic and metabolic consequences of fetal anemia. Oxygen delivery is the product of blood flow or cardiac output and arterial oxygen content, both of which are affected by hematocrit.[12] Arterial oxygen content increases with hematocrit while blood flow is inversely related to the change in hematocrit through changes in blood viscosity, which therefore makes it difficult to predict the effect of low hematocrit on oxygen delivery. Animal studies have shown that the overall oxygen delivery and consumption are decreased in anemia.[12,13] To compensate for the impaired tissue oxygenation, cardiac output increases either through an increase in heart rate or stoke volume or both in moderate-to-severe anemia, with a slight decrease in mean arterial pressure.[13,14–16] The augmented workload of the growing heart leads to cardiac hypertrophy and expansion of coronary vasculature, and eventually to cardiac decompensation in chronic severe anemia in keeping with the Frank-Starling law of cardiac functional reserve.[17,18]

Flow resistance, the ratio of blood pressure and flow, is affected by both blood viscosity and vascular hindrance.[12] Vascular hindrance describes the contribution of vascular geometry to vascular resistance and is inversely related to the radius of the vessels such that

$$R = {}^{1}\!/_{r^4}$$

where R is resistance and r is the radius of the vessel. The decrease in blood viscosity resulting from a drop in hemoglobin concentration results in lower resistance overall, which in turn contributes to the increase in blood flow velocity and cardiac output. Redistribution of blood flow to the more important organs, specifically heart and brain, has been observed in anemic animals, which is believed to be related to variation in the arteriolar smooth muscle response to circulating catecholamines in the different compartments of the fetal circulation.[12,14] Symmetrical myocardial hypertrophy has been found in chronic anemic sheep and human fetuses, which might be the result of increased cardiac workload to maintain oxygen delivery.[14,18] In combination with the dilation of arterioles and increased permeability of the small vessels, these factors are thought to lead to increased venous and capillary hydrostatic pressure and the development of hydrops fetalis. Fetal anemia and hemolysis also stimulates the extramedullary erythropoiesis in the liver and spleen, resulting in the enlargement of these two organs.[19,20] Enhanced reticulocytosis is often found in anemic fetuses as bone marrow also attempts to rescue the low red blood cell mass.[21]

Table 1. Classification of the severity of fetal anemia.

		Severity		
Definition	*Reference*	*Mild*	*Moderate*	*Severe*
Hb deviation from GA mean	Nicolaides *et al*.[22]	< 2 g/dl	2-7 g/dl	> 7 g/dl
Hb expressed as MoM	Mari *et al*.[3]	0.65 – 0.84	0.55 – 0.65	< 0.55
Hematocrit	Moise Jr and Argoti[23]		< 30%	

Hb: hemoglobin GA: gestational age; MoM: multiples of the median. Reproduced with permission from Abbasi *et al*. 2017[11]

1.1.2 Causes of Fetal Anemia

The etiologies of fetal anemia are listed in Table 2, including immune-related, infectious, genetic and other pathological conditions. Here we will focus on the common etiologies, which are also the causes of anemia in the participants of our study.

Red blood cell alloimmunization

The most prevalent cause of fetal anemia is red blood cell (RBC) alloimmunization. According to a retrospective study of 552 affected pregnancies, the incidence of RBC alloimmunization is 0.36% in the current Canadian population.[24] Historically RhD sensitization has been the predominant type, although recent studies have shown that the incidence of RhD-positive pregnancies has declined, with the highest now being RhE. This change is likely to be related to the successful treatment of RhD-sensitized pregnancies by intravascular immunoglobulin (IVIG) prophylaxis (see section 1.1.3.2) [25]. Nevertheless, RhD remains the antibody most commonly associated with the most severe cases of fetal and neonatal anemia resulting from RBC alloimmunization.[24]

The pathogenesis of fetal anemia due to RBC alloimmunization involves hemolysis of fetal red blood cells by maternal antibodies.[26] The placenta acts as a barrier preventing the passage of fetal blood cells into the maternal circulation. However, fetal red blood cells do come into contact with the maternal immune system in the setting of fetal-maternal hemorrhage during labour or as a result of placental abruption. Small numbers of fetal red blood cells also cross the placenta into the maternal circulation spontaneously during normal pregnancy. The rate of spontaneous fetal maternal hemorrhage increases with advanced gestations: 12% in the second trimester and 45% in the third trimester.[27] Incompatible fetal red blood cells activate the formation of maternal immunoglobin G (IgG) antibodies against the fetal antigen.[26] Maternal IgG antibodies can then pass through placenta into the fetal circulation, bind to the fetal red blood cell antigens and mark them for destruction by the fetal immune system, thus causing hemolytic disease of the fetus and newborn and thus anemia.

A flow diagram (Figure 1) describes an approach to the prenatal management of pregnancies with RBC alloimmunization.[2] During the first pregnancy of women with RhD (-) blood type, indirect Coombs tests are performed every four weeks to detect maternal antibodies.[28] The

indirect Coombs test is a measure of the maternal antibody titer. If the titer exceeds a critical threshold, which differs depending on the type of alloimmunization and the type of laboratory testing system used, the paternal genotype is then tested.[2] Further testing by cell free fetal DNA (cffDNA) or amniocentesis is ordered if heterozygosity for the rhesus factor or unknown genotype is found. Meta-analysis studies have demonstrated high accuracy (> 90%) of cffDNA test for RhD, RhC/c, RhE/e and Kell sensitization.[29] Upon confirmation of fetal antigen or homozygous paternal genotype, or those with previously affected pregnancies, routine MCA-PSV Doppler is performed at least once per week.[2]

Parvovirus infection

Parvovirus infection, in particular parvovirus B19, is the major non-immune cause of fetal anemia. The incidence rate of primary infection in pregnant women is low (1 - 5%) with a vertical transplacental transmission rate of 24 - 33%.[30] In addition to the anemia, other adverse outcomes in infected fetuses include profound hydrops fetalis, myocarditis associated with cardiac failure, cardiomegaly, thrombocytopenia and fetal demise.[30,31] The incidence rate of hydrops in these fetuses is only 2.9%, while 15 - 20% of all non-immune cases of hydrops are caused by parvovirus B19 infection.

Parvovirus B19 infection triggers fetal anemia by inhibiting hepatic erythropoiesis.[31] B19 is comprised by a linear, single-stranded DNA and two protein molecules. Like other DNA viruses, B19 infects human cells by an initial binding to the host cell receptors, followed by internalization and replication in the cell nucleus, and finally release of virions via cell lysis.[30] The receptor for B19 is the blood group P antigen. Although P antigen is expressed in various locations (e.g. endothelial cells and fetal myocytes), the infection occurs exclusively in the erythroid progenitor cells in the fetal liver. The peak incidence occurs in the second trimester when hepatic erythropoiesis is most prominent (Figure 2).[28,30,31] The shorter life span of fetal erythrocytes and the immaturity of the fetal immune response during this time period render the fetus more susceptible to infection.

Diagnosis of primary B19 infection involves the detection of maternal immunoglobin production in response to infection.[31] Parvovirus B19 specific immunoglobin M (IgM) is produced 7-14 days post-infection and IgG 14 days post-infection. IgM can be detected up to 6 months post-

infection while IgG persists for life-long immunity protection. Infection in fetuses is confirmed by detecting B19 DNA in the amniotic fluid or fetal blood.

Alpha-thalassemia

Alpha-thalassemia is an inherited disorder with reduced or absent α-globin chains due to mutation or deletion of one or more α-globin genes.[32] There are four α-globin genes in the human. Normal fetal hemoglobin (Hb_F) is composed of two α- and two γ-globin chains ($\alpha_2\gamma_2$) whereas adult hemoglobin (Hb_A) has two α- and two β-globin chains ($\alpha_2\beta_2$). Inactivation or deletion of one or two α-globin genes has little or no effect on α-globin chain synthesis and is usually asymptomatic. However, if three or all α-globin genes are affected, treatment is usually required. Deletion or mutation of three α-globin genes, referred to as the Hb H disease, causes moderate anemia with microcytic and hypochromic red blood cells. Hb H usually affects individuals in adult life as the excessive production of β-globin chains results in the formation of β_4 tetramer. Alpha-thalassemia major, or Hb Bart's alpha-thalassemia is the condition when all four α-globin genes are lacking, leading to the production of hemoglobin Bart's (γ_4 tetramer) instead of Hb_F starting at 8 weeks of gestation (Figure 2). The majority of affected fetuses develop hydrops fetalis and die during pregnancy or shortly after birth. Other fetal complications include cardiomegaly, intrauterine growth restriction and limb defects.[11]

The rigidity of β_4 and γ_4 tetramers and their stable cell membrane make it difficult for the red blood cells to pass through the microvasculature and also promote erythrophagocytosis, making hemolysis the major mechanism of fetal anemia in alpha-thalassemia.[32] The high oxygen affinity of the two tetramers significantly reduces oxygen delivery to the tissues. As a result, reduced oxygen delivery occurs in Bart's alpha-thalassemia with less reductions in hemoglobin concentration compared with anemia secondary to RBC alloimmunization.

Prenatal diagnosis of alpha-thalassemia can be achieved through chronic villi sampling or amniocentesis for DNA testing after 9 and 16 weeks of gestation respectively.[11] However, both procedures are related to a risk of fetal loss of about 1%. The diagnosis may be suspected through ultrasound examinations of the cardiothoracic ratio, which is an indicator of cardiomegaly, placental thickness, and hydrops. Genetic counselling in parents known with α-globin gene defects is highly recommended.[32]

Twin-to-twin transfusion/Twin anemia polycythemia sequence

Twin-to-twin transfusion (TTTS) is a chronic condition occurring in monochorionic diamniotic (MCDA) twins that is characterized by oligohydramnios in one twin and polyhydramnios in the other.[33] A few tiny, mostly unidirectional arteriovenous anastomoses in the shared placenta lead to the transfer of blood between the two twins. Twin anemia polycythemia sequence (TAPS) is a special form of TTTS, which was first described in 2007.[34] In TAPS, the donor twin becomes anemic and the recipient twin becomes polycythemic. TAPS occurs spontaneously in every 3-5% MCDA pregnancies.[33] The treatment for TTTS – laser ablation – can be associated with the development of TAPS in 2-13% due to incomplete ablation of the anastomoses. In the latter form, the former recipient usually becomes the new donor, and the ex-donor becomes the new recipient.

Several prenatal and postnatal diagnostic parameters have been suggested for TAPS, however, no uniform criteria have yet been agreed on.[33] Various guidelines have been proposed for prenatal screening of TAPS.[35] A case control study comparing 19 pairs of TAPS twins and 38 control twins showed no significant difference in the neonatal mortality and morbidity rate between the two groups.[36] TAPS pregnancies are treated with intrauterine blood transfusion for the anemic twin in combination with partial exchange transfusion for the polycythemic cotwin.[33] Spontaneous resolution may occur due to thrombosis of the arteriovenous anastomoses.

Tumors

Fetal anemia cases may occur secondary to placental chorioangiomas or hepatic hemangiomas, which are benign tumors of the placenta and liver, respectively.[37,38] The exact pathophysiology of anemia is unclear; however, the most common theories are feto-maternal hemorrhage and microangiopathic hemolytic anemia.[38,39] In both types of malformation, pregnancies with small tumors do not generally require clinical interventions, whereas large (diameter > 4-5 cm) tumors may result in fetal anemia, high-output cardiac failure, non-immune hydrops and fetal demise.

Table 2. Summary of the causes of fetal anemia.

Classification	*Causes*
Immune	
RBC alloimmunization*	Rh blood group (D, c, C, e, E) *, Kell*, Duffy (Fy^a)*, Kidd (Jk^a, Jk^b)* or any IgM RBC antibody*
Non-immune	
Congenital infection*	Parvovirus B19*, CMV, toxoplasmosis, syphilis
Inherited anemias*	Hemoglobinopathies (e.g. α-thalassemia major*), RBC membrane or enzyme disorders (e.g. G6PD deficiency, pyruvate kinase deficiency)
Bone-marrow disorders	Fanconi anemia, Diamond-Blackfan anemia
Hematopoietic malignancies	Congenital leukemia, transient myeloproliferative disorder
Fetal or placental tumors, vascular malformations, other placental pathology*	Sacrococcygeal teratoma*, liver hemangioma, hepatoblastoma, diffuse neonatal hemangiomatosis, placental chorangioma*, fetal or placental arteriovenous malformations, placental mesenchymal dysplasia
Fetomaternal hemorrhage*	Placental abruption*, trauma*
Rare genetic disorders	Lysosomal storage disorders (e.g. Niemann-Pick, Gaucher disease, mucopolysaccharidosis), neonatal hemochromatosis
Complications of monochorionic placentation*	TAPS*, cotwin demise*

*Potential candidates for intrauterine transfusion (IUT). CMV, cytomegalovirus; G6PD, glucose-6 phosphate dehydrogenase; IgM, immunoglobin; RBC, red blood cell, Rh, Rhesus; TAPS, twin anemia-polycythemia sequence. Table adapted with permission from Abbasi *et al*. 2017[11]

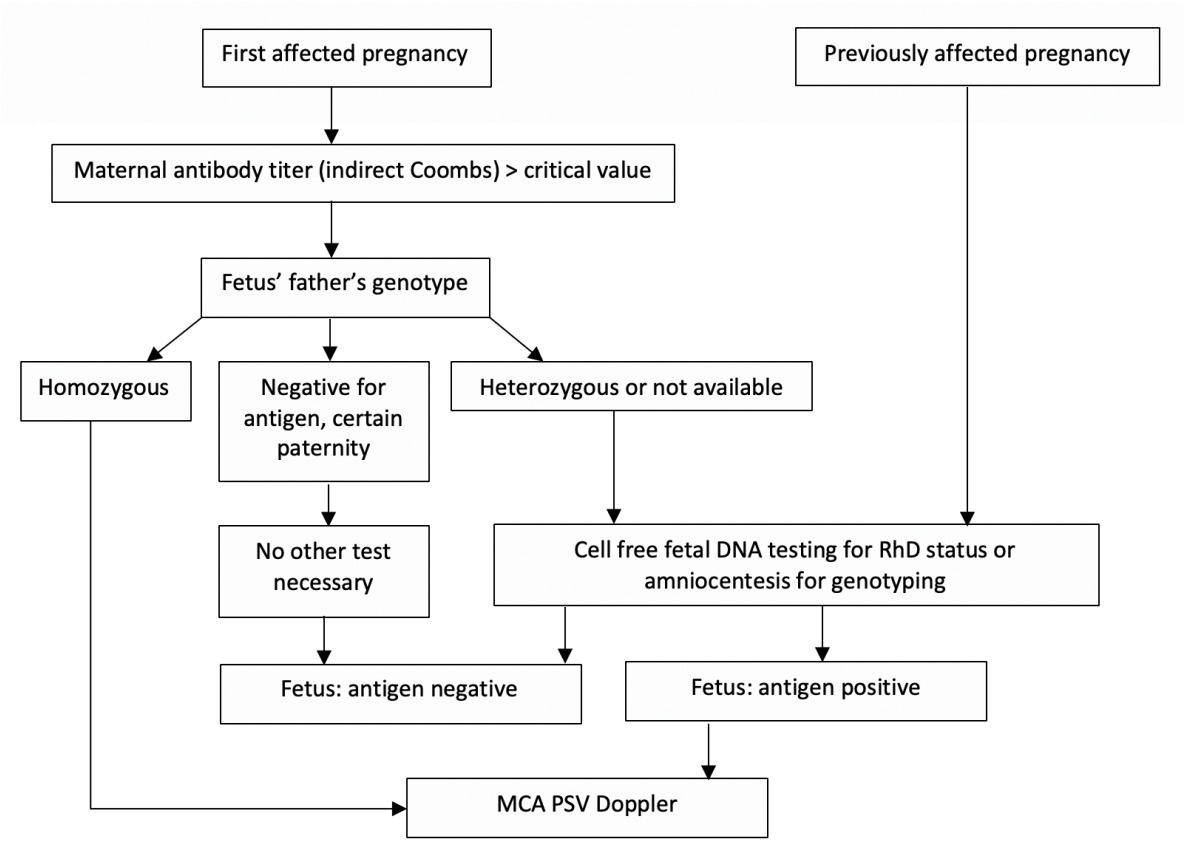

Figure 1. Algorithm for management of fetal anemia secondary to red blood cell alloimmunization.

MCA-PSV: middle cerebral artery peak systolic velocity. Figure adapted with permission from Mari *et al.* 2015.[2]

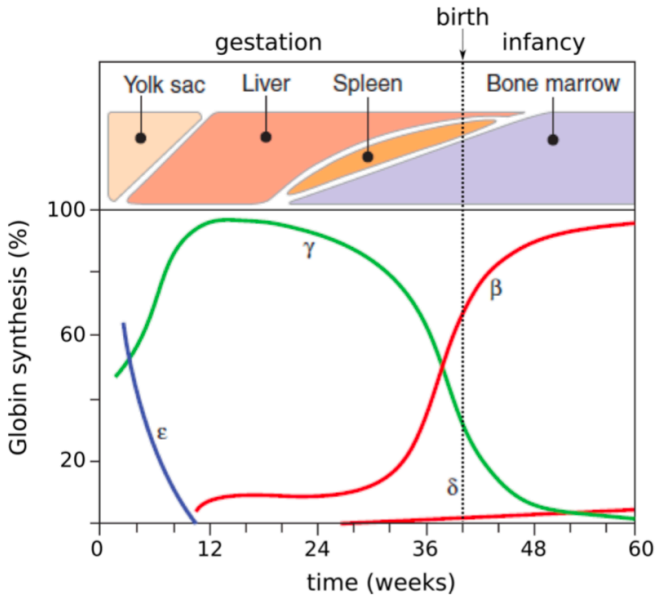

Figure 2. Synthesis of β-like hemoglobin subunits throughout gestation and in early infancy.

The predominant hemoglobin subunit during gestation is the γ-globin subunit synthesized by the liver starting from the second trimester. Synthesis of β-globin by the bone marrow increased exponentially in late gestation. Reprinted with permission from Copyright Cold Spring Harbor Laboratory Press, 2013.[40]

1.1.3 History of Fetal Therapy and Management

Although uncommon, potentially serious health consequences including fetal loss can occur if fetal anemia is not effectively diagnosed and treated *in-utero*. Given the dramatic reduction in the survival rate of anemic fetuses following the development of hydrops, the goal of managing the anemic fetuses is to identify and treat the fetuses in need of IUT treatment before the onset of hydrops.

1.1.3.1 Diagnosis of Fetal Anemia

1.1.3.1.1 Fetal blood sampling

The gold-standard technique used to diagnose fetal anemia is cordocentesis, also known as fetal blood sampling, which is the direct measurement of fetal hemoglobin or hematocrit level from

the umbilical cord.[2] Since its first description in 1979 by Rodeck and Campbell, fetal blood sampling has been used in clinic for various purposes.[4,41] In suspected fetal anemia, one to two ml of fetal blood is drawn and analyzed using standard laboratory or bedside hematology assays for pre- and post-transfusion hemoglobin concentrations. Cordocentesis is also currently the only way to diagnosis alloimmune thrombocytopenia, a condition in which the fetus has lower than normal platelets count.

Invasive fetal blood sampling is associated with procedure-related complications, the most common ones being bleeding from injection site (20 - 30%) and bradycardia (5 - 10%).[4] Other complications include infection, premature membrane rupture, abruption, preterm delivery, feto-maternal bleeding, and even worsening of anemia. Procedure-related fetal loss has an incidence rate of 1 – 2%, which is exacerbated with the presence of structural abnormalities and hydrops fetalis.

1.1.3.1.2 Amniocentesis

Amniocentesis involves the percutaneous sampling of amniotic fluid. The fluid obtained can then undergo spectrophotometric measurement to determine the concentration of bilirubin, which is proportional to the severity of fetal anemia secondary to alloimmunization. Liley was the first to report the use of amniocentesis for indirectly diagnosing fetal anemia in 1961.[42] This approach exploits the increase in fetal bilirubin and fetal excretion into amniotic fluid that results from fetal hemolysis due to red blood cell alloimmunization. The bilirubin level is estimated by measuring its absorbance at an optical density of 450 mm. The “Liley Chart” divides the absorbance level into three zones corresponding to the degree of hemolysis, where a measurement falling in Zone III indicates a requirement for immediate treatment, either by blood transfusion or delivery. However, the accuracy of the Liley Chart is limited under 27 weeks of gestation.[28] Queeran *et al* used their empirical data from fetuses studied between 14 and 40 weeks of gestation to produce an alternative chart and divided the values into four zones.[43] Studies comparing the two methods reveal conflicting results.[44,45] Furthermore, because of the nature of this method, it is only applicable in hemolytic anemia.[21] The risk associated with amniocentesis are membrane rupture, infection, feto-maternal hemorrhage (about 2.3 - 7%) and increasing severity of fetal anemia.[28,29] The procedure-related fetal loss rate is about 0.5 - 1%.[29]

In the latter part of the 20th century, amniocentesis was the major diagnostic tool for suspected fetal anemia. However, a multicenter study in 2006 comparing the accuracy of amniocentesis against MCA-PSV Doppler, led to a shift in clinical practice such that the vast majority of institutions have now abandoned amniocentesis and adopted MCA-PSV Doppler for screening fetal anemia.[46]

1.1.3.1.3 Doppler Measurements of the Middle Cerebral Artery (MCA)

Since the 1980s, researchers have looked for a non-invasive tool to manage and diagnose fetal anemia, thus avoiding the risks of amniocentesis. Ultrasound examinations of multiple fetal anatomical features, including umbilical vein diameter, head and abdominal circumferences, placental thickness, and Doppler measurements of the mean aortic blood flow velocity and blood flow in the umbilical vein either failed to show correlation with the severity of fetal anemia or had disappointing diagnostic accuracy.[47–50] The measurements of splenic and liver size and middle cerebral artery blood velocity showed more promising results.[11,20] Mari *et al* was the first to perform a multi-centre prospective study on 111 anemic fetuses with RBC alloimmunization and 265 control pregnancies to examine the correlation between MCA-PSV Doppler and the severity of fetal anemia.[3] The high sensitivity (100%) and relatively low false positive rate (12%) supported the use of MCA-PSV Doppler as a diagnostic tool for the screening of moderate-to-severe fetal anemia using 1.5 multiples of the median as the threshold. Multiples of the median, defined as the measured value divided by the expected value of the gestational age, corrects for the change of MCA-PSV throughout gestation. A small study with 16 pregnancies with RBC alloimmunization indicated the superiority of Doppler measurements over the perimeter of the spleen and liver in predicting fetal anemia.[20] Based on these and subsequent studies[17,51–54], either fetal blood sampling or induced labor will be offered when MCA-PSV Doppler is higher than the predetermined threshold or has an increasing trend (Figure 3). An example of a Doppler measurement of MCA-PSV is shown in Figure 4.

The diagnosis of fetal anemia based on MCA-PSV Doppler is supported by the evidence that the blood velocity in anemic fetuses increases as a result of lower blood viscosity and higher cardiac output.[55] The middle cerebral artery has been adopted, because it is readily identified and

interrogated in a reproducible way and because it is highly sensitive to changes in cerebral hemodynamics.

Many studies have evaluated the accuracy of MCA-PSV Doppler in diagnosing fetal anemia due to red blood cell alloimmunization. A review paper grouped the available literature published between 2000 and 2008 to determine the most appropriate criteria for the diagnosis of severe fetal anemia based on MCA-PSV cut-off values.[56] Using a cut-off of 1.5 multiples of the median, the pooled sensitivity of the MCA Doppler test was 73 - 76% and specificity was 78 – 91%, depending on the criteria used for anemia. MCA Doppler is particularly useful in Kell alloimmunization, in which neither maternal blood antibody titer nor amniotic fluid bilirubin concentration correlate well with the severity of Kell-alloimmunized anemia because the pathophysiology of Kell alloimmunization involves the destructions of red blood cell precursors but not hemolysis.[21,54,57]

The use of MCA-PSV Doppler for diagnosis of fetal anemia due to non-immune causes has also been validated. The sensitivity and specificity for anemia due to parvovirus B19 and alpha-thalassemia ranges from 85 - 94% and 89 – 93%, respectively.[53,58] The use of MCA-PSV Doppler in diagnosing TAPS has been proposed, using a cut-off of 1.5 and 1.0 multiples of the median for the anemic and polycythemic twin respectively.[59,60] The accuracy of the test in this setting was first examined by Slaghekke *et al,* who reported sensitivity and specificity for predicting anemia in TAPS pregnancies of 94% and 74%, respectively.[60] For polycythemia, the sensitivity was found to be 97% and specificity was 96%.

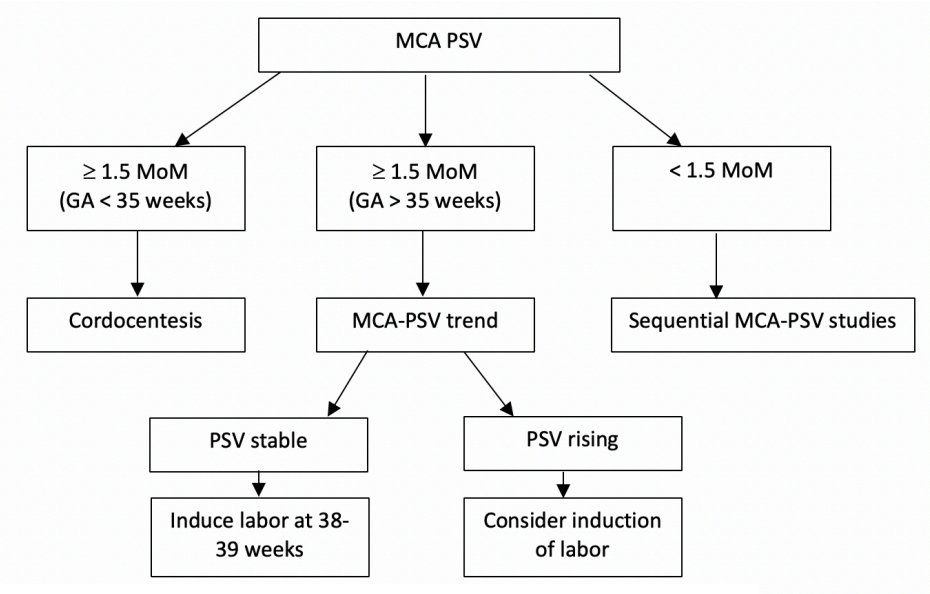

Figure 3. Management of fetal anemia using MCA-PSV Doppler.

GA: gestational age; MCA-PSV: middle cerebral artery peak systolic velocity; MoM: multiple of the median. Image adapted with permission from Mari *et al*. 2015.[2]

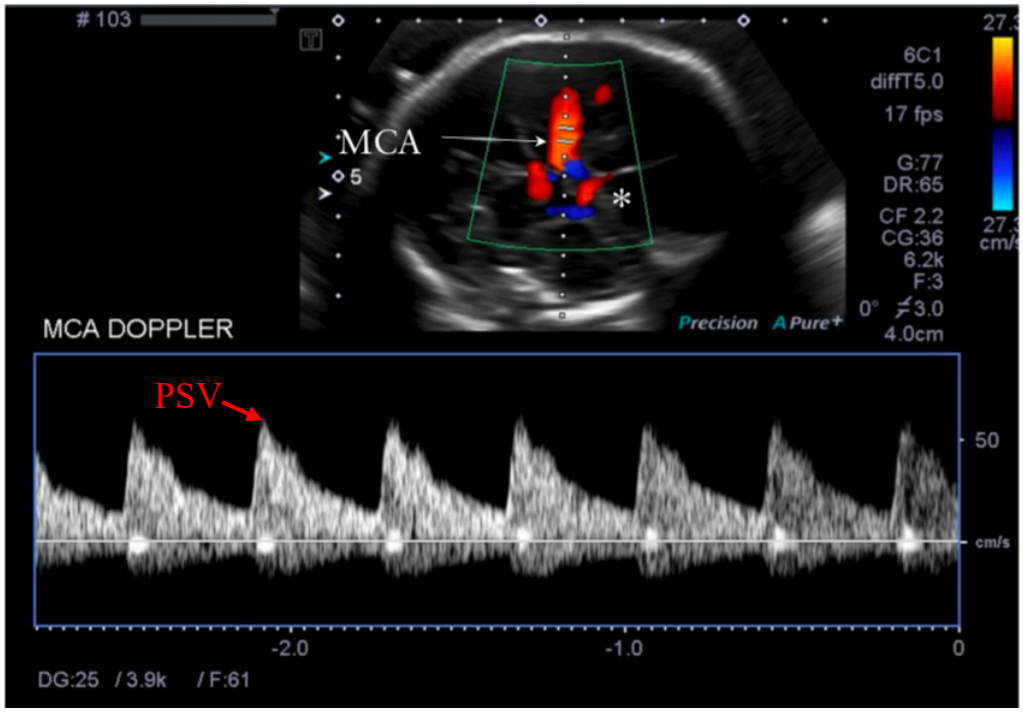

Figure 4. Example of MCA-PSV Doppler image.

MCA: middle cerebral artery; PSV: peak systolic velocity. Figure reproduced with permission from Abbasi *et al*. 2017[11]

1.1.3.1.4 Limitations of MCA Doppler

The widespread adoption of MCA-PSV Doppler in clinical practice reflects several advantages including its non-invasive nature, high accuracy in a variety of etiologies, and the easy accessibility of ultrasound. However, over the last two decades, many studies have reported problems associated with MCA-PSV Doppler. Specifically, MCA-PSV Doppler becomes less predictive after the fetus has received its first transfusion and at later gestations.

Significant correlation between hemoglobin and MCA-PSV Doppler have been reported at first, second and third blood transfusion.[6,7] Detti *et al* concluded that MCA-PSV Doppler could be used to time the second blood transfusion with high sensitivity (100%) and high specificity (94%) using a higher cut-off of 1.69 multiples of the median for severe anemia.[5] However, the specificity for detecting all fetuses who requires IUT, i.e. moderate-to-severe anemia, was only 63% using 1.32 multiples of the median as the cut-off. If this threshold was used, 17 out of 46 patients who did not require treatment would undertake the risks of fetal blood sampling. The association between MCA-PSV Doppler and fetal anemia is weaker after the second blood transfusion. In a retrospective study of 39 anemic fetuses, 5 out of 12 moderate-to-severely anemic fetuses would be missed if a threshold of 1.5 multiples of the median was used for MCA-PSV Doppler to determine the indication for the third blood transfusion.[6] Furthermore, the authors of this study were not able to provide a new threshold due to the small sample size.

A meta-analysis by Martinez-Portilla *et al* published in 2019 included 12 studies with fetal anemia due to RBC alloimmunization, parvovirus B19 and TAPS and compared the accuracy of MCA-PSV Doppler for predicting moderate-to-severe fetal anemia based on the number of transfusions received.[9] The study found no significant changes in the test accuracy using a cut-off of 1.5 multiples of the median, regardless of the number of transfusions received. The pooled specificity was relatively constant at around 72% but the sensitivity dropped from 86% (zero IUT received) to 60% (≥ 3 IUTs received). Another MCA-PSV study included 111 fetuses with hemolytic anemia and found high sensitivities for moderate-to-severe anemia even after repeated transfusions.[7] However, the specificities were only 21.9%, 50% and 50% for the first, second and third transfusions, respectively. To increase the test specificity, the authors suggested using 1.73 multiples of the median as the new threshold. The specificities did then increase to 75%, 86% and 91% while the sensitivity of MCA-PSV Doppler was compromised.

MCA-PSV measurement in later gestations is also less reliable with respect to fetal anemia. In one study, the sensitivity and positive predictive value of MCA-PSV Doppler to predict moderate-to-severe fetal anemia at 34 and 37 weeks of gestation were just 63% and 53%, respectively.[61] In addition, Zimmerman *et al* conducted a multi-centre prospective study evaluating the performance of MCA-PSV Doppler in combination with B-mode ultrasound in detecting at risk pregnancies with an intention to treat approach.[51] In pregnancies with increased MCA-PSV measurements studied before 35 weeks of gestation, the positive predictive value of detecting fetal anemia was only 53%. Furthermore, while labour was induced in seven pregnancies with elevated MCA-PSV Doppler after 35 weeks of gestation, none had more than mild anemia. Late preterm birth, defined as delivery between 34 - 37 weeks of gestations, is increasingly recognized to be associated with risks of short and long-term morbidity, including sepsis, respiratory distress, patent ductus arteriosus, impaired feeding and growth and neurodevelopmental deleay.[62]

In summary, the current standard 1.5 multiples of the median threshold of MCA-PSV Doppler has a low specificity and positive predictive value for moderate-to-severe fetal anemia, while adjusting the threshold to increase specificity lowers the sensitivity level. The limitations of MCA-PSV Doppler may result from changes in fetal hemodynamics resulting from the introduction of adult red blood cells.[5,8,11] Hb_A is smaller in size, has lower rigidity and higher propensity for aggregation compared to Hb_F, thus affecting the blood velocity in ways that are not related to the hemoglobin or hematocrit level. In addition, cerebral vascular regulation is complex and involves various factors. For example, Picklesimer *et al* found that oxygen content and partial pressure of carbon dioxide have significant influences on the cerebral vascular dynamics and thus potentially the accuracy of MCA Doppler for the detection of fetal anemia.[55] Other factors such as fetal gender, heart rate and cardiac status could also affect MCA Doppler measurements.[11]

1.1.3.2 Treatments for Fetal Anemia

1.1.3.2.1 Intravascular Immunoglobin Prophylaxis

IVIG prophylaxis is one of the non-invasive prenatal pregnancy treatments for RhD sensitized pregnancies.[63] Several mechanisms underlying the treatment effect have been proposed. On the

maternal side, the production of maternal IgG is reduced by the injected IgG antibodies through negative feedback.[19] Placental transport of maternal IgG is also affected as high level of maternal IgG saturates its placental receptors and reduces the transport ratio.[19,64] In the fetal spleen and liver, the saturation of the reticuloendothelial receptors of macrophages limits the uptake and destruction of IgG-coated fetal red blood cells.[19,63] Since its introduction in 1968, the prevalence of RhD-alloimmunized pregnancies has dropped from 2% to 0.1%.[1] In North America, IVIG is so far only available for RhD sensitized pregnancies yet RhD still affects 6 in every 1000 live births.

1.1.3.2.2 Intrauterine Blood Transfusion

The first successful case of fetal blood transfusion was reported in 1963 and was delivered to a severely anemic fetus as an intraperitoneal injection (IPT), with the transfused erythrocytes reaching the intravascular compartment via the peritoneal blood vessels and lymphatics.[65] X-ray films and contrast agent were used to locate the placenta and fetus and guide the transfusions. Since then, several improvements have been developed, resulting in a low rate of procedure-related complications. These include the use of ultrasound guidance, first reported in 1977.[28] The shift in transfusion site from intraperitoneal to intravascular (IVT) also enhanced the safety and efficiency of the procedure. Rodeck *et al* first introduced direct blood transfusions into the umbilical vein using a fetoscope.[66] In the following year, IVT into the intrahepatic portion of the umbilical vein using ultrasound guidance was introduced by Bang *et al* and gradually became the most frequently used route of administration.[67,68] Blood absorption via intra-peritoneal transfusion takes about 7-10 days whereas IVT directly transfuses blood into the fetal circulation.[2] Since hydropic fetuses have limited efficiency in absorbing blood through the lymphatic system after IPT, IVT is preferable in these cases.[66,69] The fetus appears to be protected against the development of worsening heart failure due to the rapid increase in circulating volume that might be expected with IVT by the already larger circulating volume that is intrinsic to the feto-placental circulation, whereby the placenta may serve as a large reservoir for the storage of the excess blood.[70]

Technical aspects

The current standard protocol for IUT has been described in the Society of Maternal-Fetal Medicine guidelines.[2] Briefly, cytomegalovirus-negative, O-negative, irradiated adult packed red blood cells are obtained and cross-checked with maternal blood type to minimize any adverse reaction and to assure optimal oxygen delivery. Under local anesthesia, injection is performed at the umbilical cord or the intrahepatic umbilical vein for IVT using a 20- or 22-gauge spinal needle under gray-scale or Doppler ultrasound guidance. Upon confirmation of the severity of the condition by fetal blood sampling, the obstetrician will proceed to IUT. Blood is slowly transfused to reach a final hematocrit level of 40 - 50% or hemoglobin of 15 - 17 g/ml.

Since a four-fold increase in hematocrit after IUT is predictive of a higher risk of fetal death[71], a two-step transfusion is given to severely anemic fetuses with or without hydrops.[28] For cases complicated by immune-mediated hemolytic anemia, top-up transfusions are often performed when the fetal hemoglobin level is still within the normal range to suppress the production of fetal hemoglobin antigens.[69]

Effect on fetal hemodynamics

Fetal hemodynamic changes relating to the introduction of a large volume of blood and hemoglobin are expected. Due to the non-Newtonian behavior of red blood cells, blood viscosity varies with shear rate, which in-turn depends on the vessel diameter.[72] Smaller vessels with slow flow, such as the capillaries, have low shear rate and thus high blood viscosity. Significant increases in fetal high-shear whole blood viscosity have been found post-transfusion as a result of the rise in fetal hematocrit.[73] Despite the increase in preload resulting from increased umbilical vein pressure, cardiac output drops in the immediate post-transfusion period, possibly due to the hyperviscous capillaries and resultant increase in afterload. However, after 48 hours, fetal hemodynamics appear to return to normal.

Short-term and long-term outcomes

A systematic review of 10 studies on IUT outcomes between 2006 and 2016 found an overall survival rate of about 95.5%.[63] Higher survival rates were found in fetal anemia secondary to red blood cell alloimmunization (81 – 94%) compared to other causes (67 - 77%).[74] Younger gestational age at the first transfusion and a higher number of successful IUTs are associated with higher survival rates.[75] The development of hydrops, however, negatively impacts perinatal

outcomes. Survival rate following IUT amongst alloimmunized pregnancies with hydrops fetalis is 74 - 89% and severe hydrops at the first transfusions and persisting hydrops post-transfusions are predictive of poor perinatal outcome.[16,75,76] Alloimmunized neonates often experience neonatal anemia and require top-up transfusions in the first three months of life as a result of the suppression of erythropoiesis by IUT.[11]

Overall, the long-term neurodevelopmental outcomes of children exposed to IUT treatment for RBC alloimmunization is good, with 81 – 100% of infants having normal results of developmental testing.[77] The incidence of major neurodevelopmental impairment (NDI) varies from 0 – 7.9%. The LOTUS study is by far the largest study reporting on neurodevelopment following fetal anemia, with 291 participants ranging from 2 to 17 years old.[78] The study found that the incidence rate of major NDI was 4.8%, with NDI associated with hydrops, the number of IUT performed, preterm birth < 32 weeks of gestation and severe neonatal morbidity. Harper *et al* confirmed that long-term outcome was worse with the development of hydrops, with two deaths and six major NDI occurring in 16 hydrops survivors.[79] Small studies investigating the outcome of fetuses with parvovirus B19-induced anemia and RBC alloimmunization showed a risk of major NDI of 0 – 12.5%.[80] The pathogenesis of the long-term NDI in anemic and hydropic fetuses is as yet unclear.

Little is known regarding long-term cardiovascular outcomes following fetal anemia and IUT. Smaller left ventricular mass was found in children exposed to RBC alloimmunization and IUT at a mean age of 10 years old.[77] Altered left ventricular geometry was confirmed by a retrospective study of adult survivors at a mean age of 33 years old.[81] Their left ventricular wall was also thicker compared to the normal sibling group. In addition, lower myocardial perfusion and altered vascular tone might suggest impaired coronary endothelial function due to fetal anemia and IUT.

Procedure-related complications

Despite conferring a higher survival rate in pregnancies affected by fetal anemia, IUT is an invasive procedure. Procedure-related complications include fetal bradycardia or tachycardia, membrane rupture, infection, feto-maternal hemorrhage and subsequent worsening of RBC alloimmunization, and premature delivery in cases with multiple IUTs.[28,82] In a study of 254 fetuses that underwent 740 IUTs, Van Kamp *et al* reported a total procedure-related complication

rate of 3.1% and a fetal loss rate of 1.6% per procedure.[82] A more recent review of 8 studies from 2006 to 2016 reported an overall risk of procedure-related complication of 2.7% per procedure with fetal loss of 0.6% per procedure.[63] The presence of anatomical abnormalities or hydrops dramatically increases the fetal loss rate (7% and 25%, respectively).[11]

1.2 Magnetic Resonance Imaging (MRI) in Fetal Research

Over recent decades, fetal MRI has been increasingly used as an adjunct to ultrasound to aid in the diagnosis and management of human fetal conditions in both second and third trimesters. As a result of the intrinsically different physics that enable the acquisition of images by the two modalities, MRI can provide complementary information about fetal wellbeing. Potential advantages of MRI include a greater sensitivity to different tissue characteristics and physiological properties, which have been helpful in the assessment of the fetal body and brain.[83] Over recent years, technological advances have also resulted in the feasibility of fetal cardiovascular assessment with MRI, including investigation of the potential of MRI to provide direct information about fetal and placental oxygenation.[84–86]

MRI uses a static magnetic field and radiofrequency (RF) waves to generate images.[87] Magnetic field strength is measured in Tesla (T). The most commonly used magnetic field strengths currently used in clinical practice are 1.5T and 3T. To understand how MR relaxometry might be used to estimate hematocrit, it is necessary to explain the concept of relaxometry and how it is measured, and also to discuss the relationship between the composition of blood and its magnetic properties.

1.2.1 Physics of MRI Relaxometry

Most MRI relies on the magnetic properties of the nucleus of the hydrogen atom, or proton.[87] As a result of the uneven number of particles in its nucleus, the proton has angular momentum, which results in its intrinsic property of precession or spin. The precession of this positively charged nucleus results in a small magnetic field called a magnetic moment. Although the nuclei

of other atoms also possess this property, hydrogen atoms are the most clinically relevant as they naturally exist in abundance in water and fat in the human body.

The net magnetization within the human body is the sum of the magnetic moments of all the constituent protons. Normally, these protons adopt random orientation, thus the net magnetization in the system is zero. When placed in a static external magnetic field B_0, the protons, or spins, align either parallel (low energy state) or anti-parallel (high energy state) to the applied magnetic field (Figure 5). At equilibrium, there are more spins in the low energy state compared to those in the high energy state, forming a net magnetization M_0 in the same direction as B_0. By convention, the direction of B_0 is designated as the longitudinal, or z-axis. The equilibrium magnetization, M_0, is therefore considered longitudinal. As described by the Bloch equation, any distribution of the net magnetization away from the longitudinal axis, will result in "rotation" or "precession" of the net magnetization about B_0 at the Larmor frequency ω_0, which is dependent on the strength of the external magnetic field

$$\omega_0 = \gamma B_0$$

where γ is the gyromagnetic ratio of the proton.[88]

Excitation

To detect magnetization, the equilibrium magnetization M_0 is tipped to the transverse plane (i.e. the x-y plane, perpendicular to B_0) where it processes and can be measured by a detector (i.e. receiver coil).[87] This process is known as excitation (Figure 6). RF pulses emitted by the RF coil are the energy source used for tipping spins out of alignment with B_0. The RF pulse produces a magnetic field B_1 (perpendicular to B_0) that oscillates at the Larmor frequency of ω_0. The resultant magnetization in the x-y plane is referred to as the transverse magnetization M_{xy}. The net magnetization M after RF pulse transmission is the sum of the longitudinal and transverse magnetization components.

Following an RF pulse, the resulting angle between the net magnetization, M and z axis, or the flip angle α, depends on the RF pulse duration (t_p) and the strength of B_1: $\alpha = \gamma B_1 t_p$. An RF pulse that generates $\alpha = 90°$ is referred to as a 90° pulse. Doubling either the strength of B_1 or t_p would generate a 180° pulse, and the resultant M would be antiparallel to B_0 and equal to - M_0.

Relaxation

Once the RF pulse is switched off, the net magnetization will return to equilibrium through a process called relaxation. Relaxation consists of two simultaneous processes: longitudinal and transverse relaxation, which are characterized by two separate time constants, T_1 or the longitudinal relaxation time, and T_2 or the transverse relaxation time. These two relaxation processes can also be described using longitudinal or transverse relaxation rates R_{1or2} (s^{-1}) = $1/T_{1or2}$.

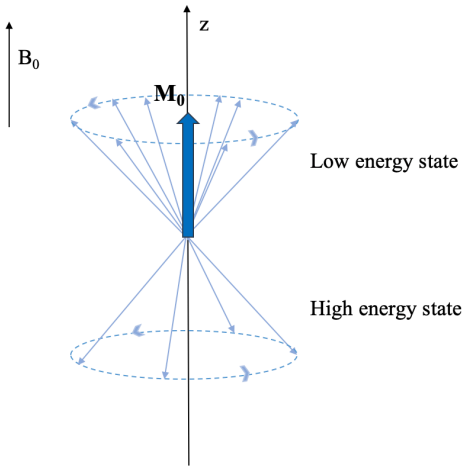

Figure 5. Spin system at equilibrium with a net magnetic field M in an external magnetic field B_0.

Spins aligned with the B_0 are at their low energy state, whereas spins aligned against B_0 at high energy state. The net magnetic field of the spin system is M_0, with the same direction as B_0.

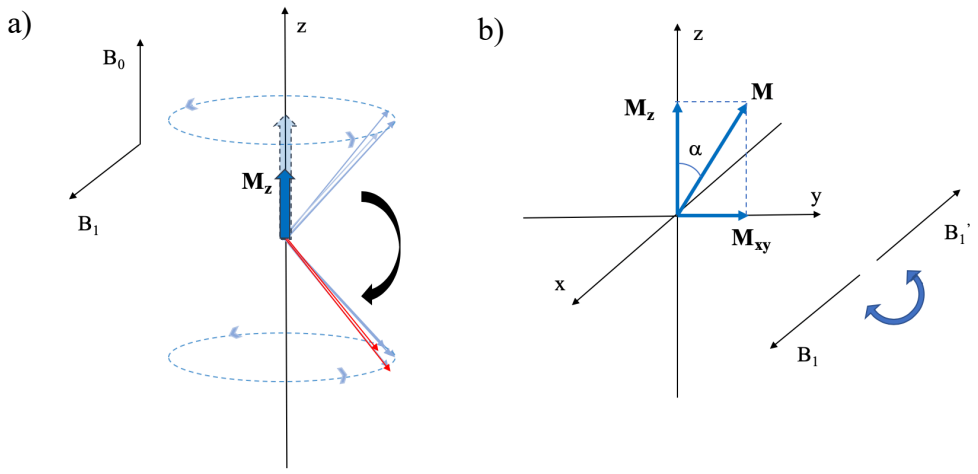

Figure 6. Excitation of spins due to RF pulse.

a) Consequences of RF pulse: two spins (red) flipped from low to high energy state, reducing longitudinal magnetization M_z; the synchronization of spins; b) The new net magnetization field M is the sum of M_z and M_{xy} (transverse magnetization). B_0 – main magnetic field, B_1 – RF pulse magnetic field.

1.2.1.1 Longitudinal Relaxation

Longitudinal relaxation is the process of energy loss from the spin system to nuclei and molecules in the surrounding environment and is dependent on the strength of the main magnetic field B_0. As energy is emitted from the spin system, the spins tend to return to their equilibrium state, resulting in the net longitudinal magnetization M_z recovering towards M_0. The longitudinal relaxation time-constant, T_1, describes the speed of the recovery process. At a time, $t = T_1$, M_z will have reached 63% of M_0 (see Appendix I Equation 1). It takes about 3-5 T_1 for full recovery to M_0 (Figure 7).

The main mechanism of longitudinal relaxation is dipole-dipole interaction. The exchange of energy between the spin system and the surrounding environment is most efficient when spins are exposed to magnetic fields fluctuating at the Larmor frequency. Therefore, the T_1 of a tissue is shorter when there is a larger portion of nearby molecules rotating or tumbling near the Larmor frequency, ω_0. Pure water molecules rotate much faster than ω_0 resulting in a longer T_1. Macromolecules in tissue, such as proteins, shorten T_1 via 'binding' of water molecules and

subsequently reducing the tumbling frequency. Providing they have rotational frequencies at or near ω_0, paramagnetic substances can further shorten T_1 because of their unpaired electrons, which have a larger magnetic moment compared to protons, and thus are more effective at inducing relaxation.

1.2.1.2 Transverse Relaxation

Transverse relaxation describes the process of decay of transverse magnetization, M_{xy}, to zero. Transverse relaxation, or T_2 decay, occurs due to dephasing of the spins (or loss of phase coherence) with no energy loss (see Appendix I Equation 2). At a time, $t = T_2$, 37% of the transverse magnetization M_{xy} is left (Figure 7). T_1 recovery is always longer compared to T_2 decay. Some sources of T_2 relaxation include the dipole-dipole interaction (which is the primary T_1 recovery mechanism) and field inhomogeneity. Dipole-dipole interactions cause alterations in the spins' orientation in the transverse plane and thus substances that affect T_1 relaxation might also change T_2 relaxation.

The local magnetic field experienced by each spin is a combination of the main magnetic field B_0 and the magnetic moments of its neighboring nuclei. The local field thus differs among spins. According to $\omega_0 = \gamma B_0$, the resultant precession frequency would differ, resulting in faster T_2 relaxation. In reality, the transverse magnetization decay occurs much faster than T_2 due to the additional inhomogeneity of the main magnetic field, B_0. The transverse relaxation time as a result of dipole-dipole interactions, local magnetic moments, as well as B_0 inhomogeneity mechanisms is noted as T_2^*. While it cannot be entirely eliminated, the B_0 field inhomogeneity is not desirable as it does not contain any physiological information.

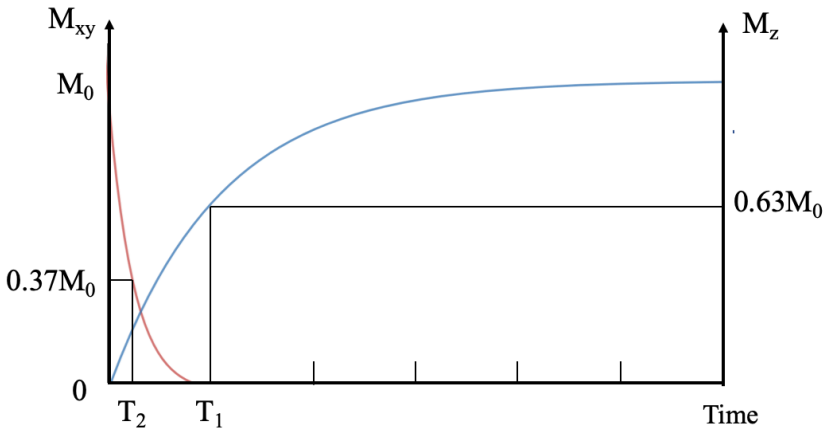

Figure 7. T_1 and T_2 relaxation as a function of time.
T_1 recovery curve in blue, T_2 decay curve in red. T_1 is time when 63% of M_0 is recovered. T_2 is the time constant when M_{xy} falls to 37% of M_0.

1.2.2 Measuring Longitudinal and Transverse Relaxation in Fetus

While conventional MRI exploits the differences between the T_1 and T_2 relaxation of tissues to create tissue contrast, there is also a field of MRI concerned with the direct quantification of T_1 and T_2 known as relaxometry.[89]

T_1 mapping

The gold-standard method to measure the T_1 of a tissue is to generate T_1 maps using an inversion recovery pulse sequence.[90] The first step of an inversion recovery sequence is a 180° RF pulse to invert the magnetization. When the pulse is switched off, the magnetization starts to recover back to equilibrium. A 90° pulse is used after a delay, called the inversion time (TI), for signal acquisition in the transverse plane. The inversion recovery measurement is repeated at several different TIs until sufficient time points are sampled during the recovery of magnetization. A time delay (of several seconds) between each measurement ensures that the magnetization is fully recovered before each new 180° pulse. The acquired data are then fitted into the T_1 recovery equation (see Appendix I) for estimation of the T_1 time constant.

A short scan time is crucial for fetal imaging to minimize the potential for gross fetal in-plane and through-plane motion during data acquisition. The most widely used sequence for efficient T_1 mapping is the modified Look Locker inversion recovery (MOLLI) that was first described by Messroghli *et al*.[91] MOLLI consists of a single non-selective inversion pulse followed by a train of balanced steady-state free precession (SSFP) acquisitions at R-R intervals during recovery.

Multiple inversions with different TIs are usually applied to sample additional points along recovery. The original description of MOLLI consisted of 3 acquisitions following the first and second inversion pulses and 5 acquisition after the last inversion pulse with each inversion separated by 3 recovery beats.[91] This pattern can be noted as 3(3)3(3)5. Deviations from the original pattern have been proposed to further shorten the scan time, including 5(3)3 and 5(1)1(1)1. MOLLI has been shown to be highly reproducible.[90] The MOLLI pulse sequence used in this study will be described in details in Section 2.

With a MOLLI acquisition, the measured T_1 time constant is not the true T_1 of stationary tissue and thus requires correction. This is because the magnetization M_z is disturbed by the repeated SSFP acquisition and cannot fully recovery even after a very long recovery period. In flowing blood, however, correction is not needed. All spins covered by the RF coil will experience the non-selective inversion pulse. However, the signal from each acquisition originates from 'fresh' blood flowing into the imaging plane that is not affect by any previous SSFP excitations.

T_2 mapping

The gold-standard method for the quantitative measurement of T_2 is T_2 mapping using a spin-echo pulse sequence.[92,93] The spin-echo sequence consists of a 90° pulse followed by a series of 180° pulses. As previously described in Section 1.2.1, all spins are in-phase immediately following the 90° excitation pulse, but then start to dephase. Starting at time $t = \tau_{180}/2$, a series of "refocusing" 180° pulses are applied at regular "refocusing intervals", τ_{180}, which serve to reverse the effects of B_0 inhomogeneity. A train of signal-maxima, or echoes, occur at $t = \tau_{180}$, $2\tau_{180}$, …, $N\tau_{180}$, and the amplitude of these echoes decays with the time constant, T_2.

In the fetus, efficient T_2 mapping is performed using a T_2 prepared SSFP sequence. The T_2-preparation step consists a non-selective spin-echo sequence (see above), followed by a tip-up - 90° pulse, which stores T_2-decayed magnetization on the z-axis for subsequent sampling by an

SSFP sequence. Similar to the fetal T_1 measurements, a series of T_2-preparation sequences, with varying T_2-preparation times T_{prep}, are each followed by an immediate balanced SSFP acquisition. The number of refocusing pulses during each preparation time is equal to T_{prep}/τ_{180}. The T_2 relaxation time is then estimated by fitting the acquired signal from each measurement versus T_{prep}. Detailed description of the T_2-preparation sequence used in this study will be presented in Section 2.

1.2.3 Relationship of T_1, T_2 and Blood SaO_2 and Hematocrit

When considering the T_1 and T_2 of whole blood, the magnetic properties of the blood can be viewed as the sum of the properties of two components or compartments where the water resides: red blood cells and the plasma.[92] This is referred to as the two-compartment model of blood. The T_1 and T_2 of plasma are mostly affected by the dissolved proteins (e.g. albumin, globulins) and water, and less so by dissolved O_2. For erythrocytes, the magnetic properties change depending on the oxygenation state of hemoglobin. Deoxyhemoglobin, the form of hemoglobin with no oxygen bound, has four unpaired electrons, and is therefore paramagnetic. This means that a higher content of deoxyhemoglobin will hasten both T_1 and T_2 relaxation.

T_1 and T_2 relaxation for whole blood are affected by the quantity of hemoglobin in blood (hematocrit, Hct) and the percentage of hemoglobin bound with oxygen (oxygen saturation or SaO_2). T_1 or R_1 of whole blood is simply the weighted sum of the two components:

$$R_{1,blood} = Hct \cdot R_{1,ery} + (1 - Hct) \cdot R_{1,plas}$$

$$= Hct \cdot \left(R_{1,ery} - R_{1,plas}\right) + R_{1,plas}$$

R_1 of erythrocyte, in turn, relies on the SaO_2 as follows:

$$R_{1,ery} = R_{1,ery,0} + (1 - SaO_2) \cdot r'_{1\ dHb}$$

where $R_{1,ery,0}$ is the relaxation rate of fully oxygenated erythrocyte and $r'_{1\ dHb}$ is a constant that describes how relaxation is affected by deoxyhemoglobin concentration. T_2 relaxation is similar to T_1 but slightly more complex. On top of the individual T_2 of the two components, the difference in the magnetic field between erythrocyte and plasma exacerbates the field

inhomogeneity of whole blood. Spin exchange between the field-shifted plasma and erythrocytes thus leads to a shortening of T_2. An additional parameter, $R_{2,ex}$, that depends on hematocrit, oxygen saturation and the refocusing interval of the T_2 mapping sequence, is therefore added to the equation:

$$R_{2,blood} = Hct \cdot R_{2,ery} + (1 - Hct) \cdot R_{2,plas} + R_{2,ex}$$

The relationship between $R_{2,ery}$ and SaO_2 is similar to that of $R_{1,ery}$:

$$R_{2,ery} = R_{2,ery,0} + (1 - SaO_2) \cdot r'_{2\ dHb}$$

There is a strong linear relationship between the R_1 of blood and its hematocrit. For the transverse relaxation of whole blood, the magnetic field difference between erythrocytes and plasma ($R_{2,ex}$) is responsible for giving rise to the classic quadratic relationship between SaO_2 and T_2.

In summary, hematocrit is the major determinant of blood T_1 while T_2 depends most on SaO_2. T_1 is inversely related with hematocrit, and lower SaO_2 slightly shortens T_1 (Figure 8). T_2 increases with SaO_2 whereas hematocrit shortens T_2 with a stronger effect at higher SaO_2 (Figure 9).

The dependence of MR relaxation properties on blood SaO_2 and hematocrit in adult blood has been studied at various field strengths, including 1.5, 3 and 7 T.[86,93–96] Only recently was the MR relaxometry of fetal blood characterized at 1.5 and 3 T to serve as a reference for future calibration.[86,97] Fetal blood has several important differences from adult blood that could alter the relaxation times of erythrocytes and plasma. Firstly, as mentioned in Section 1.1.3.1.4, the more globular fetal RBC is bigger in size compared to the bi-concave adult RBCs.[98] Secondly, fetal plasma is less viscous due to the lower protein content in plasma.[99] Thirdly, the membrane of a fetal RBC is about 50% less permeable to water.[100] This influences the spin exchange between the plasma and erythrocytes compartments. Finally, the fetal hemoglobin has a higher affinity for oxygen, which contributes to the exchange of oxygen from the maternal to fetal blood.[73] Our group previously found that fetal blood has shorter T_1 and longer T_2 compared with adult blood for a given hematocrit and SaO_2 level at 1.5 T.[86] The T_1 of fetal blood collected from the umbilical cords of babies delivered electively at term by caesarian section is shorter at 1.5T than

at 3T as T_1 changes proportionally with the external field strength.[86,97] By contrast, T_2 is shorter at 3T.

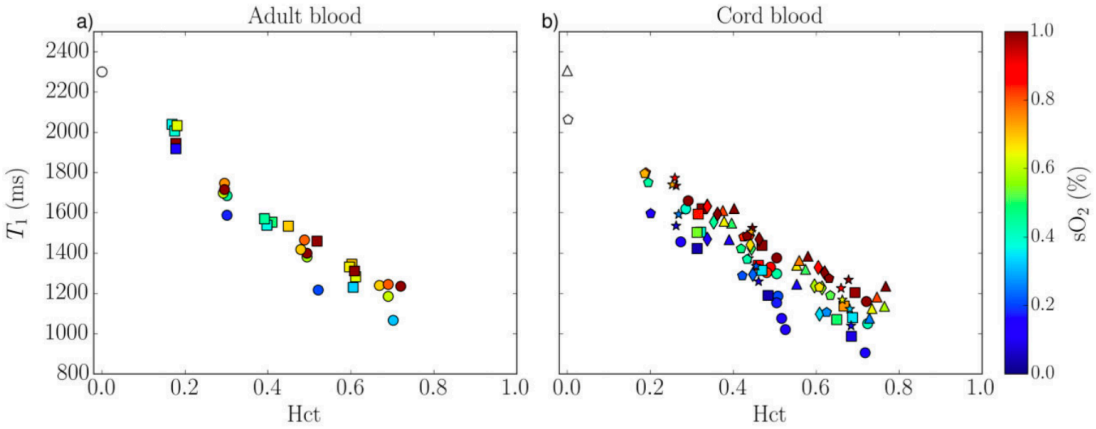

Figure 8. T_1 relaxation time as a function of hematocrit (Hct) in a) adult and b) cord blood.

Data points are colour coded by oxygen saturation (sO_2). Images adapted with permission from Portnoy *et al.* 2017.[86]

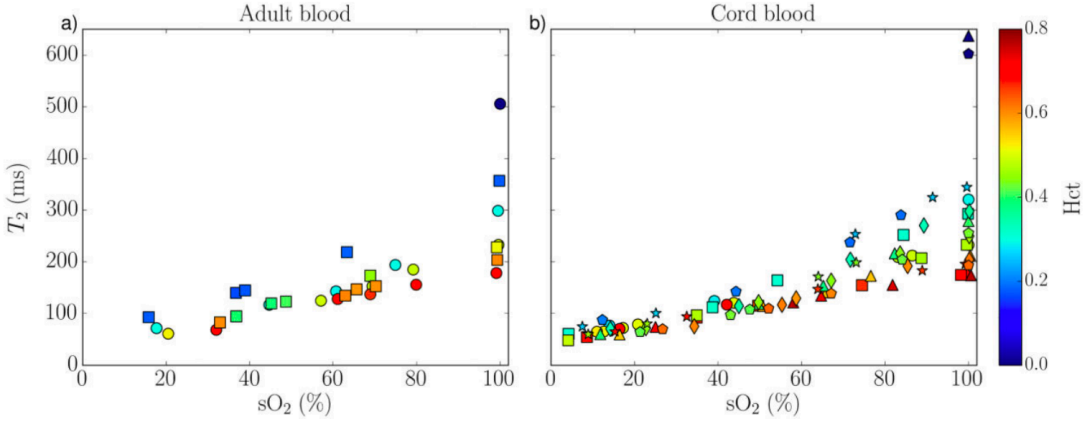

Figure 9. T_2 relaxation time as a function of oxygen saturation (sO_2) in a) adult and b) cord blood.

Data points are colour coded by hematocrit (Hct) level. Images adapted with permission from Portnoy *et al.* 2017.[86]

1.2.4 Non-invasive Measurement of Hematocrit *in vitro*

As we have outlined above, the measurement of fetal hematocrit and SaO2 is conventionally undertaken by invasive fetal blood sampling, which carries a risk of fetal loss of 1-2%. However, through an understanding of the relationship between MR relaxometry and blood hematocrit and oxygen saturation, T_1 and T_2 mapping has provided the possibility of estimating hematocrit and SaO2 *in utero* in a quick and non-invasive manner. Previously, T_2 mapping has been validated *in vitro* and *in vivo* in studies that aimed to estimate fetal SaO_2.[84,85,101]

The *in vitro* validation of MRI to estimate the hematocrit of umbilical cord blood on a 1.5T MR system was first reported by our group in 2017.[101] MOLLI and T_2 preparation sequences were used in this study to acquire T_1 and T_2 relaxation measurements from blood manipulated through a range of SaO_2 and hematocrit using variable exposure to nitrogen gas and hemodilution or hemoconcentration and then imaged in test-tubes placed in a water bath maintained at body temperature and intermittently agitated. MRI derived SaO_2 and hematocrit measurements were compared with conventional blood gas analysis measurements performed immediately after imaging.

As seen in the previous section, the longitudinal and transverse relaxations are determined by both hematocrit and SaO_2. Each relaxation rate constrains the range of possible hematocrit and SaO_2 values within the physiological range (Figure 10). For a given pair of T_1 and T_2 (or R_1 and R_2) values, the intersection(s) of the two curves would be the solution(s) for hematocrit and SaO_2. The following cubic polynomial equations are used to solve for hematocrit and SaO_2:

$$G_0 \cdot (Hct)^3 + G_1 \cdot (Hct)^2 + G_2 \cdot (Hct) + G_3 = 0$$

$$H_0 \cdot (SaO2)^3 + H_1 \cdot (SaO2)^2 + H_2 \cdot (SaO2) + H_3 = 0$$

where $G_{0,1,2,3}$ and $H_{0,1,2,3}$ are determined by the measured R_1 and R_2 of the whole blood, and the parameters of the two-compartment model (e.g. $R_{1,ery}$, $R_{1,plas}$, $r'_{1,dHb}$…) at a given magnetic field strength. With the T_1 and T_2 measurements obtained from the blood sample, it is possible to use the equations to solve for hematocrit. In this study, the authors estimated hematocrit and SaO_2 using the above equations with the two-compartment model parameters obtained from cord blood. The results showed that the bias between the predicted and true blood hematocrit was only 0.011, with an uncertainty of ± 0.1.

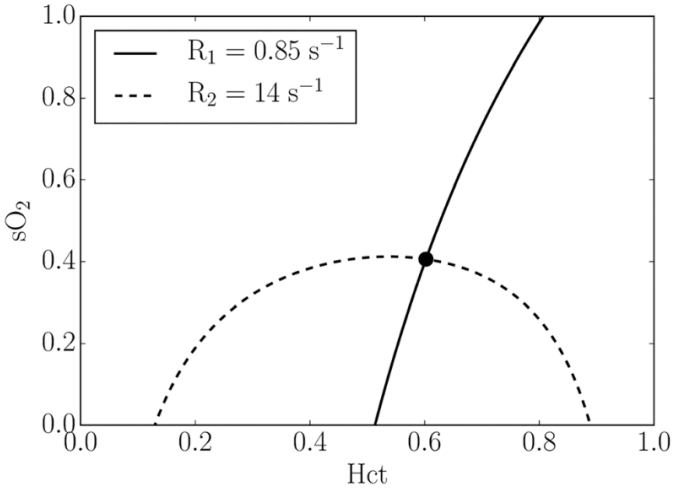

Figure 10. Hematocrit (Hct) and oxygen saturation (sO_2) constrained by T_1 and T_2 measurements.

Image adapted with permission from Portnoy *et al*. 2017.[101]

2 Rationale and Objectives

Fetal anemia is evaluated noninvasively by MCA-PSV Doppler. However, the existing literature suggest that MCA Doppler has higher likelihood of being falsely-positive after the fetus has received IUTs and also in late gestation. This is important because the inaccurate MCA-PSV measurements might expose the patients to the potential of unnecessary and risky fetal blood sampling. This highlights the need for a complimentary diagnostic test. A previous *in vitro* study showed that hematocrit can be estimated using MRI T_1 and T_2 relaxation times.

The overall goal of this study was to investigate the feasibility and accuracy of MRI for estimating hematocrit *in vivo* in suspected fetal anemia by comparing MRI with MCA-PSV Doppler and the conventional hematological analysis of fetal blood samples. The objectives of this study were therefore as follows:

Objective 1: To determine the accuracy of MRI to estimate fetal hematocrit by comparing the MRI measurements against the laboratory hematocrit from the gold-standard fetal blood sample.

Objective 2: To test the accuracy of MRI in detecting moderate-to-severe anemia compared to MCA-PSV Doppler, specifically the sensitivity, specificity, positive and negative predictive values and the test accuracy.

3 Method

The study was designed as a prospective cross-sectional study comparing MRI measurements against fetal blood sampling and MCA-PSV Doppler measurements in fetuses with suspected anemia. It was approved by the Research Ethics Board at Mount Sinai Hospital (REB15-0267-A) and the Hospital for Sick Children (REB 1000051457) in Toronto, Canada. Funding was provided by a Health Research Grant from the Physicians' Services Incorporated Foundation.

3.1 Target Population

Pregnant women in their second or third trimester who were 18 years of age or over and scheduled for intrauterine fetal blood transfusion or fetal blood sampling for suspected fetal anemia or thrombocytopenia at the Fetal Medicine unit at Mount Sinai Hospital, were invited to participate in our study. Women with contraindications to MRI were excluded. Written consent was obtained from all participants. The results of the MRI scans were not used to guide the patients' clinical treatments. However, if incidental findings were found that were not identified through clinical examinations, the participant and the responsible physicians or staff were notified.

The main focus of our study was the anemic fetuses, although we included polycythemic fetuses in pregnancies complicated by twin anemia-polycythemia sequence and fetuses with thrombocytopenia whenever they underwent fetal blood sampling.

3.2 MRI Protocol

3.2.1 MRI Scan

Participants were scanned on a clinical 1.5 Tesla MRI system (Siemens Avanto, Erlangen, Germany) at the Hospital for Sick Children. Prior to the scan, all participants completed an MRI Safety Questionnaire. Participants were free to lie on the scanner table in a position of their choice, i.e. lateral or supine, with a body matrix coil covering the maternal abdomen and a spine

coil embedded in the patient table. Lateral position was preferable to prevent maternal hypotension due to inferior vena cava compression.

Anatomical images of the fetus were acquired in the sagittal, coronal and transverse planes to localize the umbilical vein (Figure 11). Based on these images, ungated T_1 and T_2 mapping sequences were acquired in the short axis of the intrahepatic umbilical vein using a MOLLI and a T_2 preparation pulse sequence respectively. Both sequences employed with a single-shot SSFP acquisition for the readout. The MOLLI sequence consisted of two inversions with 7 inversion images acquired per inversion for a total of 14 inversion times, ranging from 100 to 5600 ms (Figure 12). As described in Section 1.2.2, T_1 correction was not required in flowing blood. The preparation times for the T_2 sequence were 32, 64, 128, 160 and 192 ms, using a 16 ms refocusing interval τ_{180} (Figure 13). The T_1 inversion times and T_2 preparation times were selected to span the expected T_1 and T_2 relaxation times of the umbilical vein.

Both sequences ran on the sequence default "untriggered" mode. The R-R interval, RR_{eff}, is determined by the $TI_{start,max} + T_{bSSFP}$ and $T_{prep,max} + T_{bSSFP}$ for T_1 and T_2 mapping, respectively.[92] The recovery period, T_{REC}, between subsequent inversions or T_2 preparation was approximately 8 seconds to ensure a short scan time while allowing for full recovery of the magnetization to equilibrium. Other MRI sequence parameters are listed in Table 3. The scan time for T_1- and T_2-measurements was approximately 30 and 24 seconds, respectively.

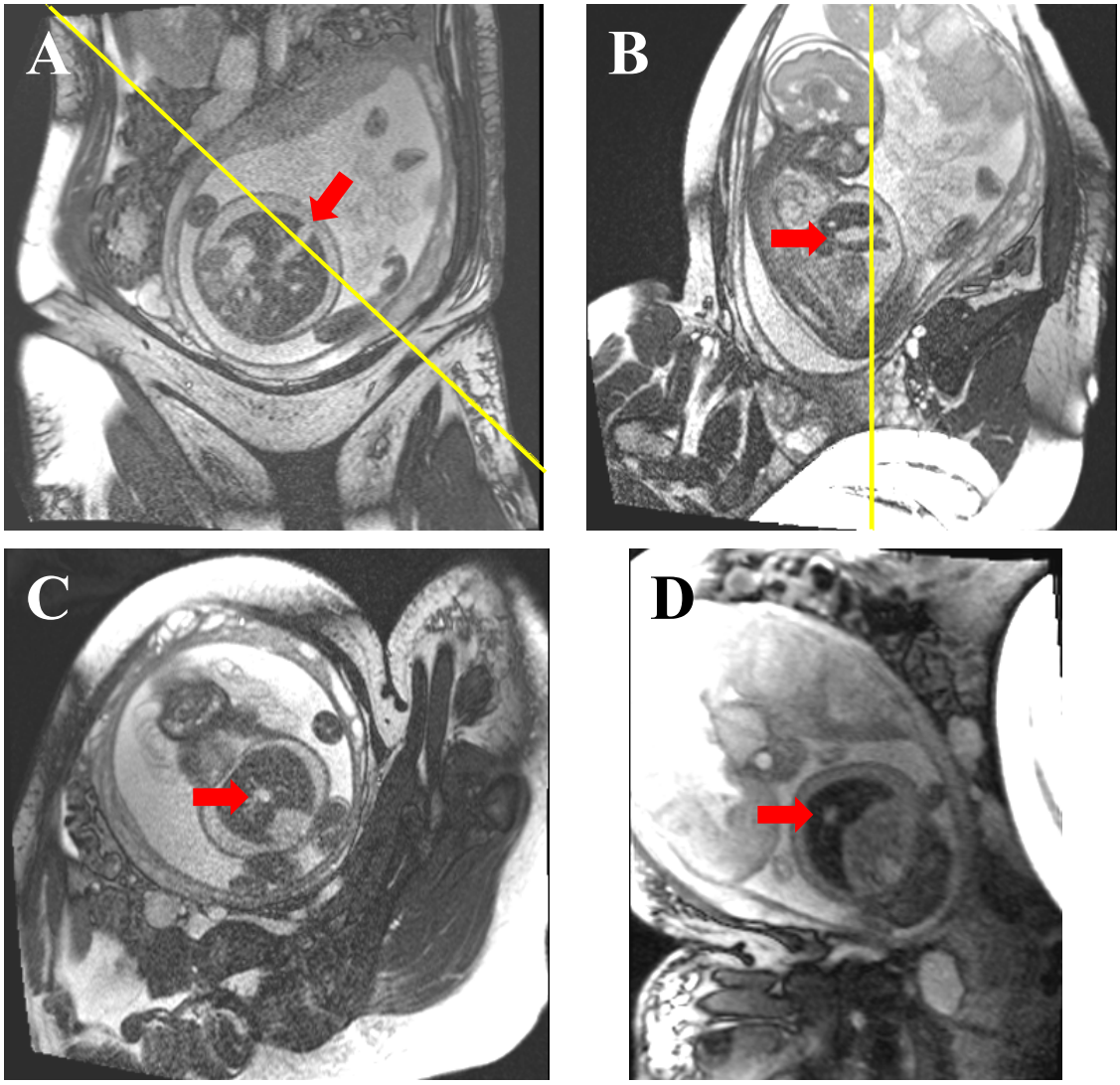

Figure 11. Example of fetal anatomical images in three orthogonal planes.

Images of the fetus in the A) transverse, B) sagittal and C) coronal orientation were used to localize the umbilical vein. D) The resulting T_1 image of the umbilical vein was acquired by prescribing the slice perpendicular to the intrahepatic portion of the umbilical vein in the transverse and sagittal planes. Red arrow: umbilical vein. Yellow line: slice prescription reference line.

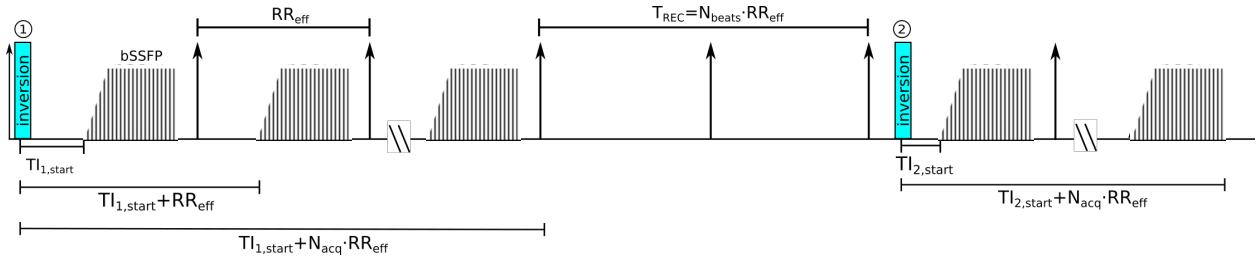

Figure 12. Pulse sequence diagram for ungated Modified Lock-Locker Inversion Recovery (MOLLI) sequence.

The sequence includes two non-selective inversions of magenetization (coloured boxes), each followed by seven balanced steady-state free precession (bSSFP) acquisitions that sample the recovering magnetization at regular intervals, $TI_{start} + N_{acq} \cdot RR_{eff}$, where $0 \leq N_{acq} \leq 7$. The sequence runs on a default "untriggered" mode with a period $RR_{eff} = TI_{start,max} + T_{bSSFP}$, where T_{bSSFP} is the duration of the SSFP acquisition and $TI_{start,max}$ is $TI_{1,start}$. The last acquisition from the first inversion and the start of the second inverion is separated by a recovery period, $T_{REC} = N_{beats} \cdot RR_{eff} = 16 \cdot RR_{eff}$. Image modified with permission from Portnoy, Sharon: Fetal Magnetic Resonance Oximetry (Doctoral Dissertation). Retrieved from: http://hdl.handle.net/1807/91949.[92]

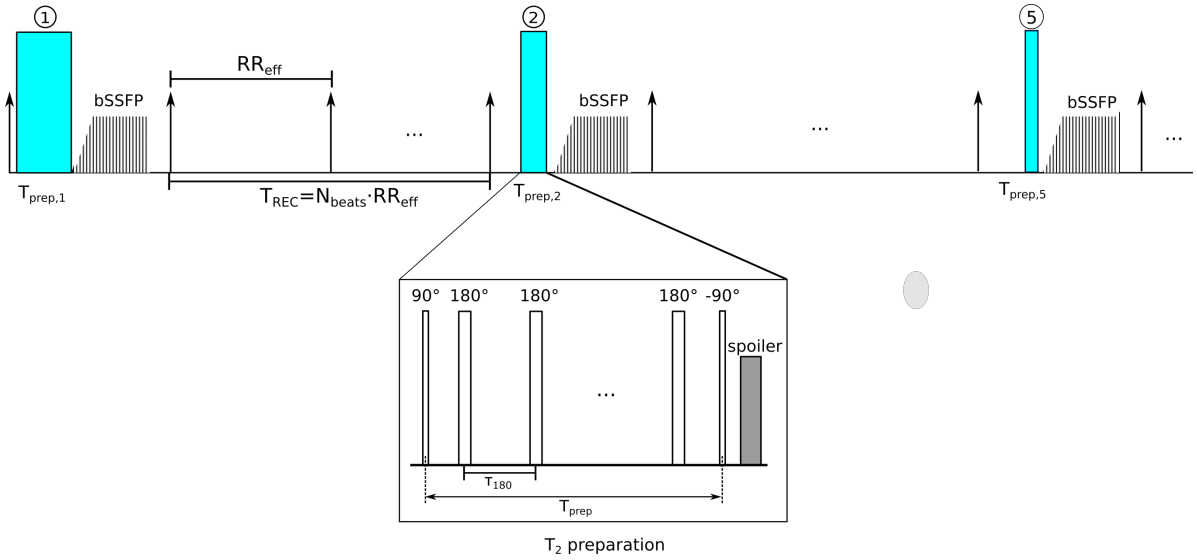

Figure 13. Pulse sequence diagram for ungated T_2-preparation sequence.

The sequence includes five T_2-preprations (coloured boxes) with different prep time (T_{prep}), each immidiately followed by a balanced steady-state free precession (bSSFP) acquisitions. The sequence runs on a default "untriggered" mode with a period $RR_{eff} = T_{prep,max} + T_{bSSFP}$, where T_{bSSFP} is the duration of the SSFP acquisition and $T_{prep,max}$ is $T_{prep,1}$. The recovery period, T_{REC}, is given by $N_{beats} \cdot RR_{eff} = 16 \cdot RR_{eff}$. The T_2 preparation module consists of a 90° pulse followed by a series of 180° pulses and a -90° pulse to tip-up the T_2-decayed magnetization. A final spoiler gradient is applied to remove any transverse magnetization. Image modified with permission from Portnoy, Sharon: Fetal Magnetic Resonance Oximetry (Doctoral Dissertation). Retrieved from: http://hdl.handle.net/1807/91949.[92]

Table 3. MRI scan protocol parameters for T1- and T2-mapping.

Sequence	SSFP Readout
TE	1.13 – 1.42 ms
TR	2.26 – 2.84 ms
Slice thickness	6 mm
Flip angle	60 - 70°
Matrix size	224 × 136
Partial Fourier	6/8
Acceleration Factor	2
FOV	350 × 280
Resolution	1.56 × 2.06 mm

SSFP: steady-state free precession, TE: echo time, TR: repetition time, FOV: field of view

3.2.2 Post-processing

The images were co-registered using non-rigid motion correction and then interpreted using lab-developed software written in Python (https://github.com/shportnoy/blood_roi_tool) to quantify T_1 and T_2 relaxation times (Figure 14).[102] To avoid partial volume effects, the regions-of-interest were manually prescribed on each T_1 or T_2 image to cover the central 60% of the umbilical vein.[103] The acquired T_1 and T_2 measurements were then used to estimate hematocrit with the equations, that were described in Section 1.2.4, calibrated for *in vitro* human fetal blood at 1.5 T.[101]

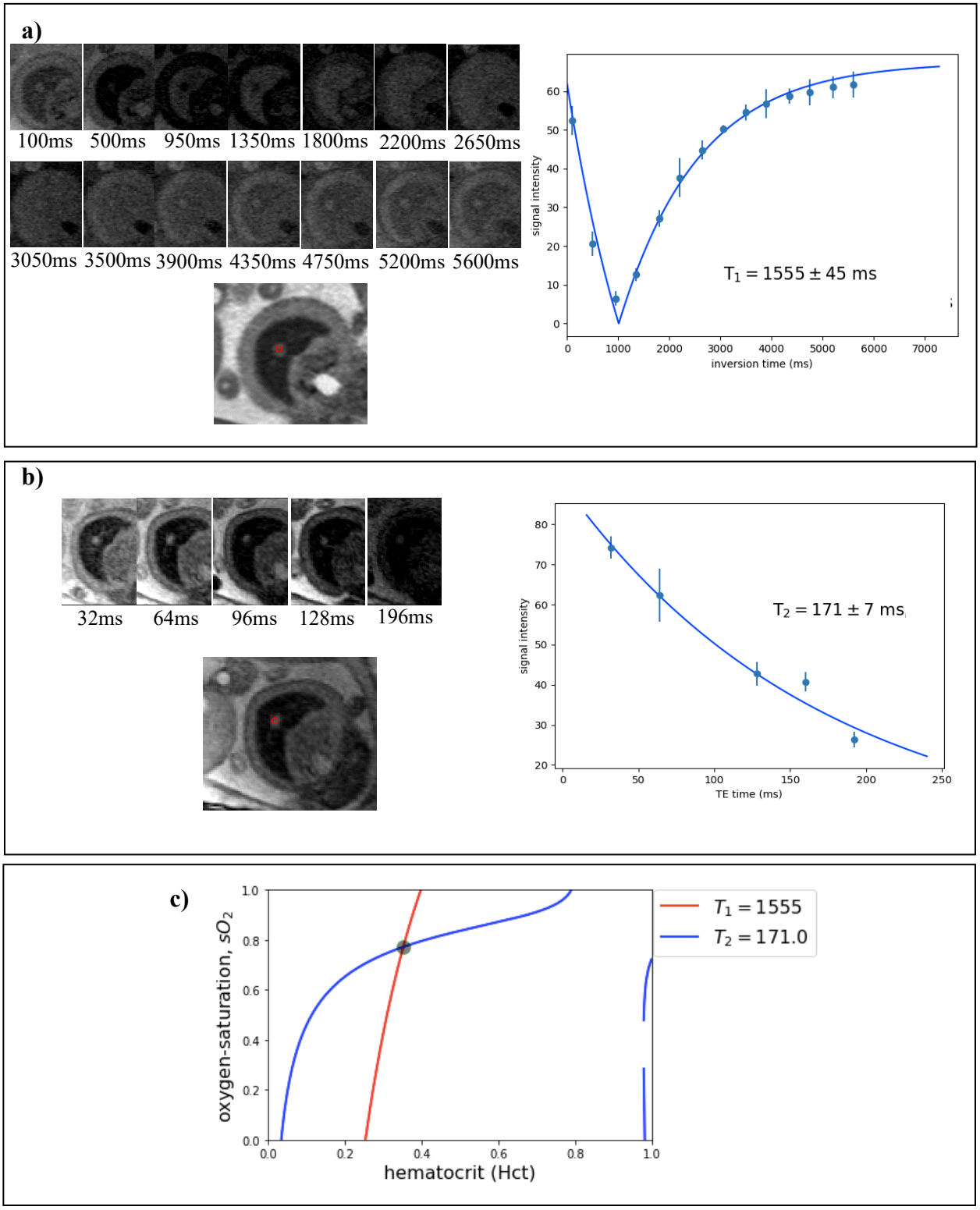

Figure 14. Example of MRI post-processing of T_1 and T_2 of the umbilical vein.
a) T_1 images (labelled by their respective inversion time TI) and T_1 recovery curve obtained using MOLLI sequence, b) T_2 images (labelled by their respective echo time TE) and T_2 decay curve using T_2 preparation sequence c) T_1 = 1555 ms and T_2 = 171 ms gave a solution of

hematocrit = 35% and oxygen saturation = 78%. The region-of-interests are shown on the bottom of a) and b).

3.3 Definition of Fetal Anemia

We adopted previously published reference ranges for hematocrit and Doppler peak systolic velocity in the middle cerebral artery to define fetal anemia.[3] The expected values of hemoglobin concentration and peak systolic velocity in the middle cerebral artery (MCA-PSV) were calculated as follows[3,104]:

$$\text{hemoglobin concentration (g/dL)} = e^{(2.84-8.55/GA)}$$

$$\text{MCA-PSV (cm/sec)} = e^{(2.31+0.046 \times GA)}$$

where GA is the gestational age (week). These equations were derived from their empirical data[3,104]. Hemoglobin concentration was converted to hematocrit based on the following general rule[105]:

$$\text{hematocrit (\%)} = \text{hemoglobin concentration (g/dL)} \times 0.03 \times 100\%$$

To adjust for the expected increases in hematocrit and MCA- PSV with advancing gestation, the reference ranges were expressed as multiples of the median corrected for gestational age[3]:

$$\text{multiples of the median} = \text{measured value/expected value}$$

Moderate-to-severe fetal anemia was defined as ≤ 0.65 multiples of the median for hematocrit, and ≥ 1.5 multiples of the median for Doppler peak systolic velocity in the middle cerebral artery.[3]

3.4 Doppler MCA, Fetal Blood Sampling and Blood Transfusion

All MRI examinations were accompanied by same day MCA Doppler examinations. The investigators making the MRI and Doppler measurements were blinded to each other's measurements. Standard MCA-PSV Doppler ultrasound was performed at Mount Sinai Hospital

before and after the transfusions using a iU22 ultrasound scanner with C5-1 transducer (Philips, Best, the Netherlands) to assess the severity of fetal anemia and to monitor the fetuses post-transfusion. Briefly, the peak systolic velocity was measured in the middle cerebral artery close to its origin from the internal carotid artery during fetal quiescence with an angle of insonation between 0° to 10°.

Under ultrasound guidance, fetal blood samples were drawn from the intrahepatic umbilical vein immediately before and after fetal transfusion for fetal hematocrit and hemoglobin concentration measurements. Upon confirmation of the presence of low hemoglobin level using HemoCue® Hb 201$^+$ system (HemoCue, Ängelholm, Sweden), transfusion would proceed. Fresh adult donor blood for transfusion were plasma reduced, irradiated, leucocyte depleted and cytomegalovirus antibody negative.[2] Donor blood was transfused intravascularly or intraperitoneally to achieve a final hematocrit of 40-55%.[1]

3.5 Statistical Analysis and Sample Size

To evaluate the accuracy of MRI, we first analyzed the correlation between the laboratory and MRI-estimated hematocrit before and after transfusion in all cases using a multilevel mixed-effects linear model. We adjusted for the repeated measurements of the same patients over time, the infrequent occurrences of multiple gestation pregnancies and the scan type (i.e. pre- or post-transfusion) to take account of the clustering within subjects and within pregnancies. Agreement between MRI and fetal blood sampling measurements was analyzed using a Bland-Altman plot. The intra- and inter-observer agreement of T_1 and T_2 was performed by JWX and JML, respectively. The measurements were obtained by prescribing the regions-of-interest on each T_1 and T_2 images while blinded to the original measurements. The agreement was then assessed using Pearson linear regression and Bland-Altman analysis. Next, we generated receiver operating characteristic curves for the pre-transfusion MCA-PSV Doppler and MRI measurements to compare their performance in identifying moderate-to-severe fetal anemia. In addition, the sensitivity, specificity, positive and negative predictive values of the pre-transfusion MCA-PSV Doppler and MRI measurements were calculated using a standard binomial proportion test. A number needed-to-treat analysis was also performed for MRI. Values are expressed as mean ± standard deviations and the statistical significance level was set at 0.05. The

data were analyzed using Stata release 15.1 (StataCorp Inc, College Station, Texas) and GraphPad Prism 7 (GraphPad Inc, San Diego, CA).

Our original sample size was determined as 40 patients to yield approximately 200 paired observations (from 100 blood transfusions) of MRI-estimated and laboratory hematocrit to detect a minimum difference of 0.3 g/dL between the two methods with an 80% power and 0.05 significance, assuming the mean and standard deviation of the difference between the two methods were 0 g/dL and 1.49 g/dL, respectively. However, recruitment was slower than we anticipated, resulting in a smaller sample size of 33 measurements in 23 fetuses. Nevertheless, despite the smaller sample size than anticipated, we were able to show a statistically significant improvement in the specificity of MRI hematocrit versus MCA-PSV Doppler as described in detail below.

4 Results

4.1 Participants

From February 2016 through August 2018, 23 women consented to participate. Of these, one participant was excluded for not undertaking a fetal blood sample and one participant was lost due to MRI scheduling difficulties. A total of 25 fetuses (five twin pregnancies and one triplet pregnancy) were scanned before and after their 1st to 4th blood transfusion or fetal blood sampling procedure for an average MRI scan time of ten minutes. In the triplet pregnancy, only the anemic and polycythemic fetuses were examined. Multiple MRI scans throughout gestation were performed for seven fetuses: four were scanned twice and three were scanned three times. Four MRI measurements from four fetuses were excluded due to unacceptable image quality resulting from excessive fetal motion. Therefore, 33 scans from 23 fetuses were included in the final analyses (Table 4). The average gestational age of the fetuses at the time of MRI was 28.4 ± 4.2 weeks (range: 19 – 36.6 weeks). Fetal diagnoses are shown in Table 4.

Table 4. Basic characteristics of the participating fetuses

Characteristics		Value
No. of participants		23
No. of multiple pregnancies		6
Mean gestational age at the time of MRI (range) – weeks		28.4 (19-36.6)
No. of participants with multiple MRI scans throughout gestation		
	Scanned twice	4
	Scanned three times	3
No. of IUT received at the time of MRI		
	0	13
	1	13
	2	5
	3	1
	4	1
No. of cases with the following etiology		
Anemia		
Red cell alloimmunization		
	Anti-D antibodies	5
	Anti-C antibodies	1
	Anti-Kell antibodies	2
	Anti-D + anti-C antibodies	1
Non-immune cause		
	Alpha-thalassemia	3
	Twin anemia polycythemia sequence (anemic)	6
	Hepatic haemangioma	1
	Chorioangioma	1
Others		
	Twin anemia polycythemia sequence (polycythemic)	2
	Neonatal alloimmune thrombocytopenia	1

4.2 MRI vs Gold-standard Fetal Blood Sampling

Figure 15 shows the MRI measurements and diagnoses of each patient at the time of MRI. There were 25 pre-transfusion (22 from suspected anemic fetuses) and 8 post-transfusion scans. Based on the pre-transfusion laboratory hematocrit, 11 fetuses with suspected anemia had moderate-to-severe anemia while the remaining fetuses were normal or had mild anemia. None of the fetuses had moderate-to-severe anemia after receiving a blood transfusion.

The MRI estimates of hematocrit ranged from 3% to 66% (Figure 16a). The mean absolute difference between the MRI-estimated and laboratory hematocrit was 6% ± 5% (range: 0.3 – 16%) with a correlation of 0.77 ($p < 0.001$) determined by the multilevel mixed-effects model. The Bland-Altman analysis showed a systematic bias of -3% (95% limits of agreement: -16 - 10%) between MRI and fetal blood sampling (Figure 16b). We found high levels of intra- and inter-observer agreement of the MRI relaxometry measurements (Appendix II Figure S1, 2).

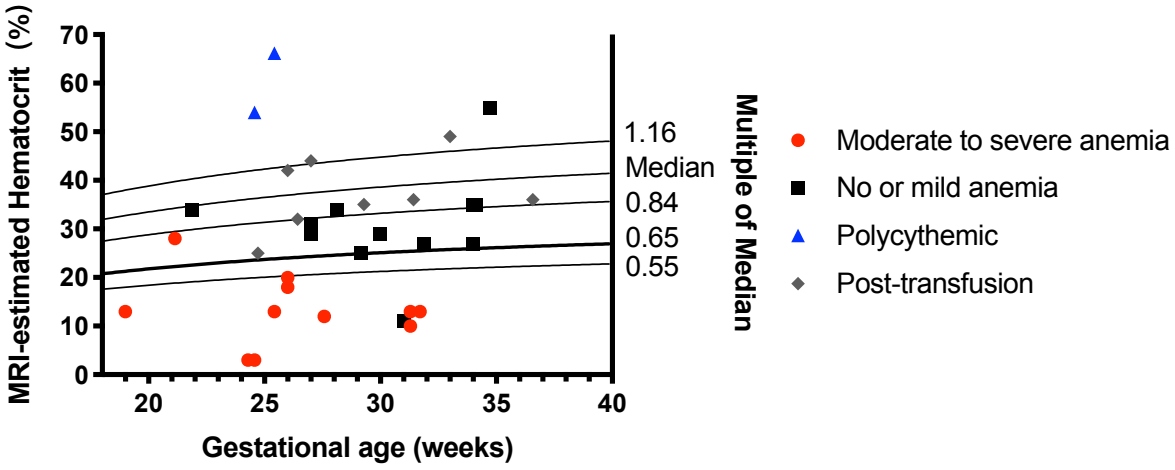

Figure 15. MRI-estimated hematocrit as a function of gestational age.

Gold standard diagnosis based on fetal blood sampling measurements before and after transfusion indicated by the symbols, showing the presence of one false negative and one false positive result by MRI (reference ranges adopted from Mari *et al*[3]: 1.16 and 0.84 multiples of the median are the 95th and 5th percentile, respectively; cut-off for moderate-to-severe anemia: 0.65 multiples of the median. Some data points represent multiple measurements of a single fetus).

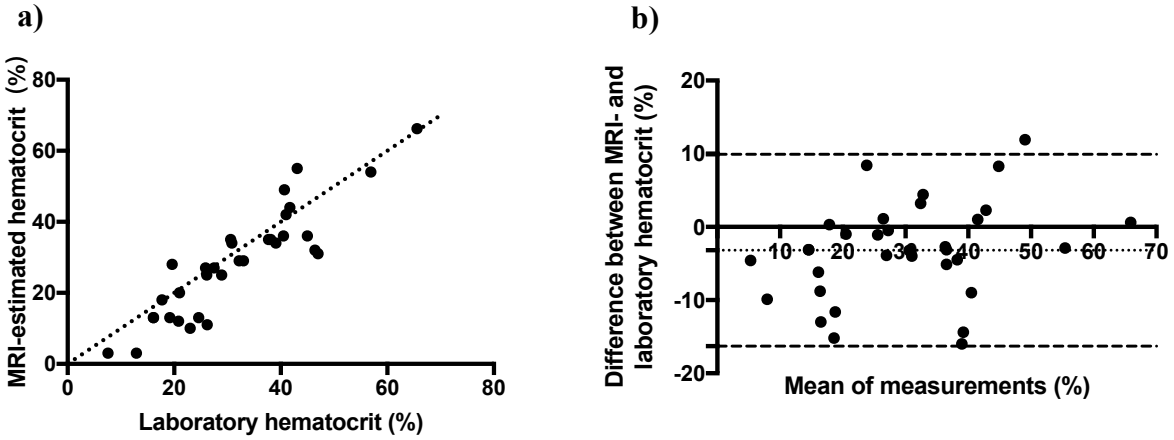

Figure 16. Comparison of MRI and laboratory measurements from 23 patients (n=33). MRI estimates of hematocrit were obtained using a combination of umbilical T_1 and T_2 measurements. Laboratory hematocrit was determined from fetal blood sampling. a) Correlation between MRI-estimated and laboratory hematocrit of 0.77 ($p < 0.001$) using a multilevel mixed-effects model (dashed line represents the identity), b) Bland-Altman analysis shows agreement between the two methods (bias = -3%) (dashed line represents the 95% limits of agreement).

4.3 MRI vs Doppler

Figure 17 compares the receiver operating characteristic curves of pre-transfusion MCA-PSV Doppler and MRI measurements. The area under the curve for the MRI measurement (0.92) was similar to that of Doppler (0.91).

The performance of MRI-PSV and MCA Doppler for detecting moderate-to-severe fetal anemia at the time of their first to fourth blood transfusions is summarized in Table 5. The positive and negative predictive values of MRI were 91% (95% CI: 59 - 100%) and 93% (95% CI: 66 - 100%), respectively. MCA-PSV Doppler had a positive predictive value of 71% (95% CI: 42 - 92%) and a negative predictive value of 91% (95% CI: 59 - 100%). MRI and Doppler had similarly high sensitivities of 91% (95% CI: 59 - 100% for both methods). The specificity of MRI was 93% (95% CI: 66 - 100%), which was 22% higher than that of Doppler (71%, 95% CI: 42 - 92%).

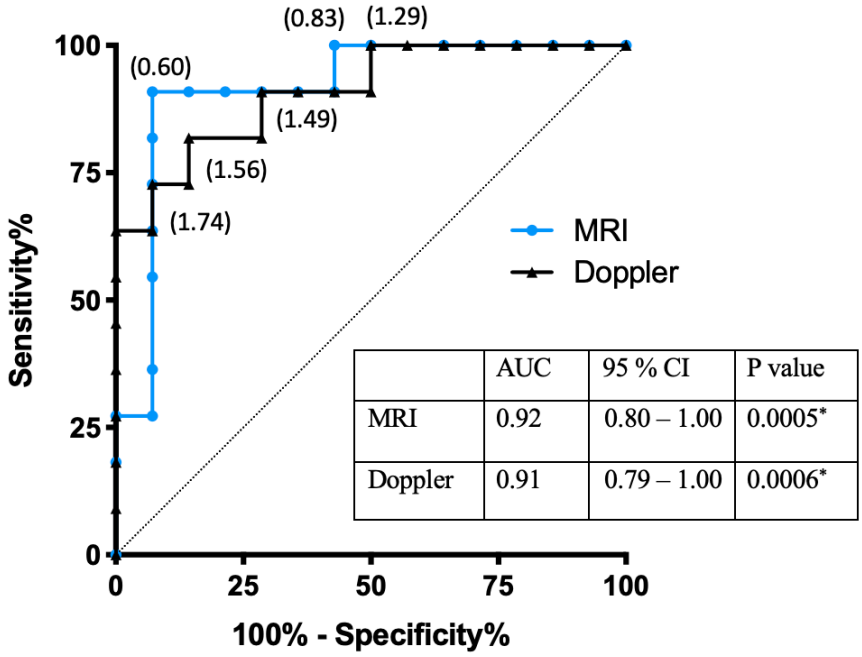

	AUC	95 % CI	P value
MRI	0.92	0.80 – 1.00	0.0005*
Doppler	0.91	0.79 – 1.00	0.0006*

Figure 17. Receiver operating characteristic curves for Doppler ultrasonography and MRI pre-transfusion measurements for the detection of moderate-to-severe fetal anemia.

Data were compared against the gold-standard fetal blood sampling measurements using a cut-off for moderate-to-severe fetal anemia of 0.65 multiples of the median.[3] Values of MRI-estimated hematocrit (multiples of the median) or Doppler middle cerebral artery peak systolic velocity (multiples of the median) are shown in brackets, with areas under curve (AUC) and corresponding p values shown. * represents significant results.

Table 5. Sensitivity, Specificity, Positive and Negative Predictive Values of All Pre-transfusion Doppler and MRI Measurements in Predicting Moderate-to-Severe Fetal Anemia at the Time of the 1st to 4th Intrauterine Blood Transfusions.

Test characteristics	Doppler	MRI
	Percent (95% confidence interval)	
Cut-off[a]	1.5 multiples of the median	0.65 multiples of the median
Sensitivity	91 (59-100)	91 (59-100)
Specificity	71 (42-92)	93 (66-100)
Positive predictive value	71 (42-92)	91 (59-100)
Negative predictive value	91 (59-100)	93 (66-100)

Data were compared against the gold-standard fetal blood sampling measurements.
a. Cut-offs were adopted from Mari *et al.* 2000[3]

4.4 Numbers Needed-to-treat Analysis

Given the 22% difference between MRI and Doppler specificity and a conservative estimation of 1% risk of fetal loss per fetal blood sampling[28], we estimated that one unnecessary fetal death could be prevented for every 450 patients with fetal anemia tested with MRI, at a cost of approximately $110,000. Assuming each moderate-to-severely anemic fetus receives one blood transfusion (a significant underestimate), at least 1400 fetal blood samplings are performed every year in the US.[3] Thus, we have estimated that approximately three unnecessary fetal losses per year could be prevented with the use of MRI in the US alone.

5 Discussion

In this study, we present a novel non-invasive method for the detection of moderate-to-severe fetal anemia. Our results suggest that MRI is accurate for estimating hematocrit in the setting of fetal anemia, with a significantly higher specificity than MCA-PSV Doppler ultrasonography. Our data supports the use of MRI to confirm the need for fetal blood sampling due to the high positive predictive value for the need to perform fetal blood transfusion.

Hematocrit has a strong negative linear relationship with T_1.[86,94] After adjustment for repeated measurements, multiple gestations pregnancies and the scan type, the MRI-estimated hematocrit showed good correlation and excellent agreement with fetal blood sampling, even as early as 19 weeks of gestation. This is in keeping with the results of a recent study by Jorgensen *et al* where T_1 of the umbilical vein was shown to predict moderate-to-severe fetal anemia in 11 normal and 8 anemic fetuses.[106] However, as far as we are aware, our study is the first to use MRI to estimate fetal hematocrit *in vivo*, and confirms that this is possible with a high degree of accuracy across a wide range of gestational ages and hematocrit levels.

5.1 T_1 Mapping in Fetuses

We have previously demonstrated the feasibility of T_2 mapping in human fetal vessels to estimate oxygen saturation in late gestation, applying the principles established by Stainsby and Wright to avoid partial volume artifacts.[103,84,85] The results of this study confirm the feasibility of undertaking T_1 mapping in the umbilical vein using a similar approach. Stainsby and Wright recommended using a region-of-interest covering the central 60% of the vessel diameter and a slice thickness less than the vessel diameter to minimize measurement errors in the quantitative measurement of blood's T_2.[103] The diameter of the umbilical vein is 5-6 mm at 24 weeks of gestation and increases to 10 mm by 40 weeks, so the central 60% of the vessel diameter has a diameter of approximately 3-4 mm at 24 weeks and 6 mm at 40 weeks.[107] With a voxel size of 1.6 mm, the sample volume is therefore comprised of between 2 and 4 voxels. A region-of-interest of this size may result in low signal-to-noise ratio.[103] Furthermore, contrary to the recommendations provided by Stainsby and Wright, the slice thickness used in our study (6 mm) is greater than the vessel diameter in the second trimester, while obtaining a slice exactly

perpendicular to the long axis of the vessel of interest can be challenging due to fetal motion and curvature of the vessel. Collectively, these issues theoretically reduce the accuracy of MRI for estimating fetal hematocrit at earlier gestations due to partial volume artifacts. Despite these challenges, we obtained diagnostic images as early as 19 weeks of gestation, confirming the feasibility of T_1 mapping across a clinically-relevant gestational age range, especially for severe fetal hemolytic anemia. Our technique is, however, particularly suited to estimating hematocrit during the third trimester, when the target fetal vessel is much larger, and MCA-PSV Doppler has a lower positive predictive value for fetal anemia.

Hematocrit can also be estimated using T_1 and SaO_2 if the SaO_2 values are obtained (see Appendix I Equation 3).[92] To test the potential of using T_1 and SaO_2 to estimate hematocrit, the same analyses of the multilevel mix-effects model and Bland-Altman were performed to compare MRI hematocrit estimate using SaO_2 and T_1 and laboratory hematocrit (Figure 18). Assuming the SaO_2 of umbilical vein is 0.8 or 80%, the MRI estimates of hematocrit still show great correlation of 0.71 and similarly low bias of -3%, despite that the actual SaO_2 ranged from 45% - 99%. The absolute difference between MRI and laboratory measurements was also similar (6%).

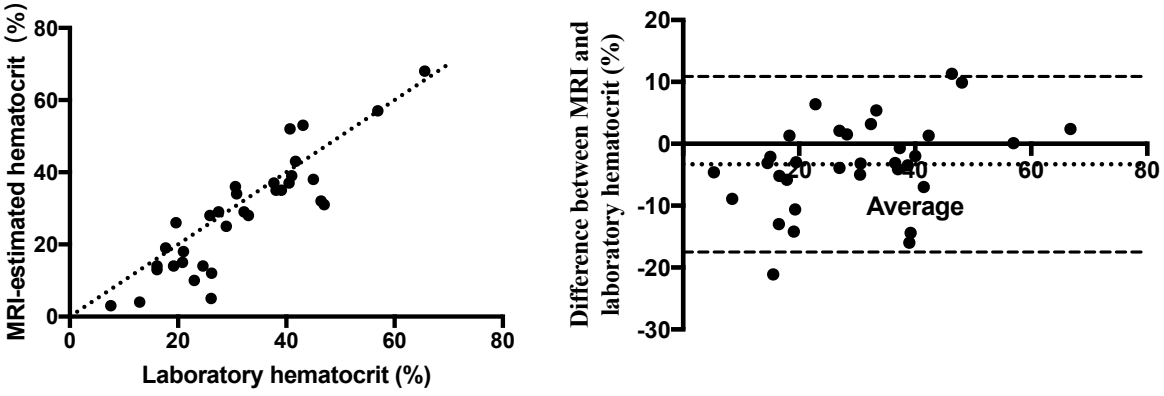

Figure 18. Comparison of MRI estimates of hematocrit from SaO_2 and T_1 and laboratory measurements from fetal blood sampling from 23 patients (n=33).

a) Correlation between MRI-estimated and laboratory hematocrit of 0.71 ($p < 0.001$) using a multilevel mixed-effects model (dashed line represents the identity), b) Bland-Altman analysis shows agreement between the two methods (bias = -3%) (dashed line represents the 95% limits of agreement).

5.1.1 T_1 Calibration

As mentioned in Chapter 1.2.2, the T_1 relaxation time of umbilical cord blood is consistently shorter (by up to 10%) than that of adult blood at the same hematocrit and oxygen saturation levels.[86] This is potentially important because after each transfusion, the proportion of fetal hemoglobin in the fetal circulation decreases as adult hemoglobin increases. The decrease of fetal hemoglobin post-transfusion is usually dramatic because 1) the transfused adult hemoglobin is physiologically more stable, and 2) because transfusion also suppresses the fetal erythropoiesis from the bone marrow, and 3) because some maternal antibodies passively enter the fetal circulation as the needle inserts into the umbilical cord through the maternal abdomen, destroying more fetal hemoglobin.[108,109] Mari *et al* reported that after the first and second transfusion, the proportion of fetal hemoglobin could range from 3 - 82% and 0 – 34%, respectively using the Kleihauer-Betke test.[6] Therefore, using a calibration based on fetal blood to estimate hematocrit may introduce inaccuracies following repeated transfusions.

In order to assess the impact of variations in relative proportions of adult and fetal hemoglobin on the accuracy of fetal MRI-estimated hematocrit measurements, we first compared the relationship between T_1 and hematocrit using calibrations based on *in vitro* analyses of the magnetic properties of fetal and adult blood. As expected, we found a significant difference in the intercept but not the slope of the T_1 and hematocrit relationship when using a fetal versus an adult calibration ($p< 0.001$, Figure 19a). Hemoglobin electrophoresis results showed that in our patients, the mean proportion of fetal hemoglobin decreased from 86% before any transfusion to 3.9% after the second transfusion (Figure 19b). However, we were reassured to find that despite the changes in hemoglobin composition, the use of a fetal- or adult-derived calibration did not result in a statistically significant difference (average difference of 6% and 7% respectively) in the accuracy of MRI-estimated hematocrit measurements, regardless of the number of transfusions received (Figure 19c), supporting the use of a calibration based on fetal blood, even after two blood transfusions.

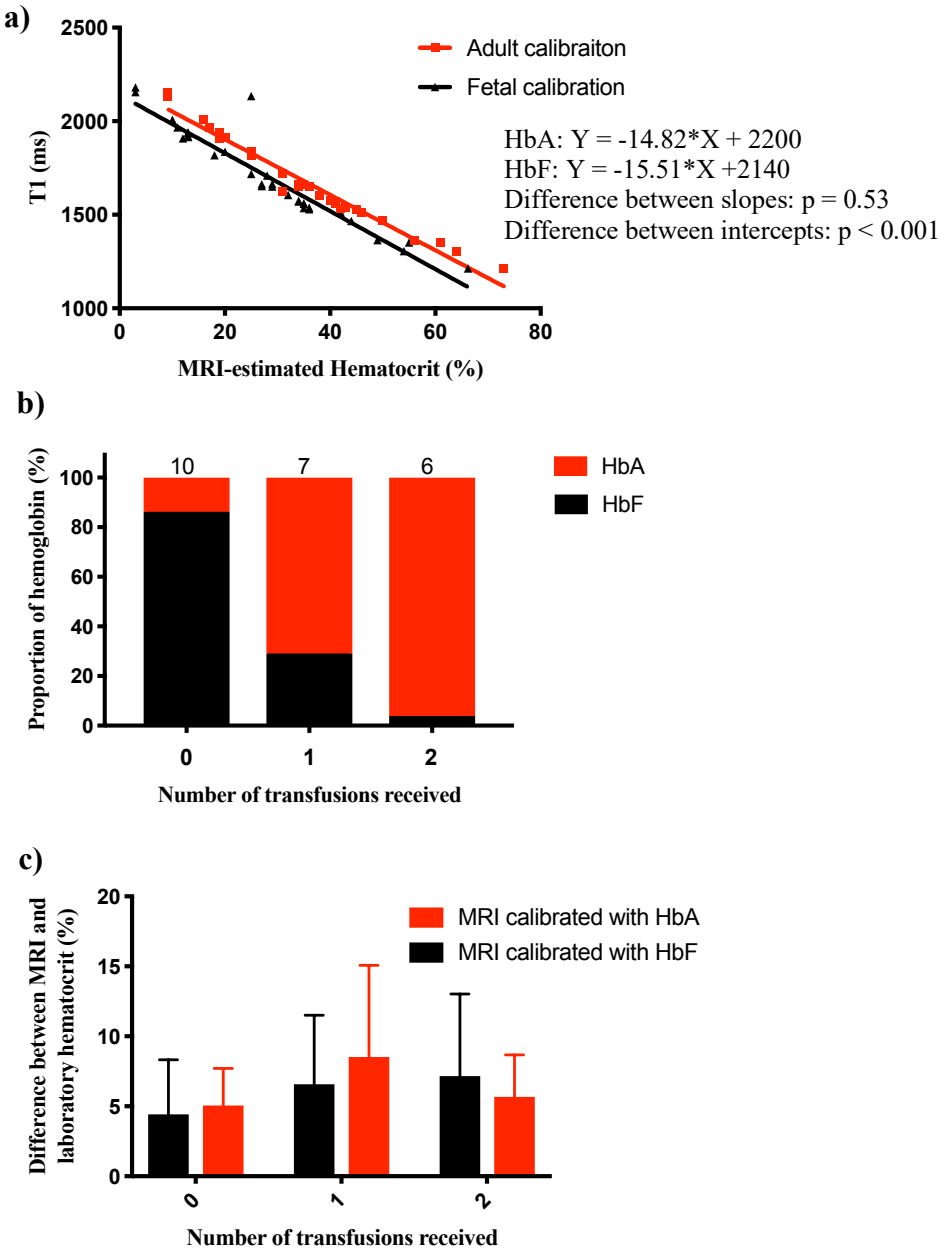

Figure 19. Investigation of diagnostic impact of using fetal versus adult calibration for hematocrit from MRI relaxometry.

a) T_1 plotted against MRI hematocrit using either fetal (black) or adult (red) calibration. p values of the differences between the slopes and intercepts are shown. b) Proportion of fetal (HbF, black) or adult (HbA, red) hemoglobin depending on the number of transfusions received. Number of data points are shown on the top of the bars. c) Difference between MRI and laboratory hematocrit depending on the number of transfusions received were calculated by either using fetal (black) or adult (red) calibration for MRI measurement. Mean and standard deviation (if applicable) are shown.

5.2 Comparisons with Previous Studies

In a meta-analysis, the overall pooled sensitivity and specificity of MCA-PSV Doppler were 79% and 73%, respectively.[9] However, most of the studies included in this review were retrospective. Here, we compare our results with three large prospective multi-center studies on the performance of MCA-PSV Doppler for detecting fetal anemia using 1.5 multiples of the median as the cut-off (Table 6). The presence of the anemia was determined by fetal blood sampling or cord hemoglobin level at birth, using hemoglobin < 0.65 multiples of the median for moderate-to-severe anemia[3,51] or > 5 SDs[17] for severe anemia. Similar to our results, all three studies reported high sensitivities and negative predictive values and relatively low positive predictive values. However, the specificity of Doppler (71%) in our study was lower than previously reported, which may have been due to our inclusion of fetuses with causes of anemia other than alloimmune-mediated hemolysis, or the relatively small sample size of our study (as discussed in more details in Chapter 5.3 below). Nevertheless, the specificity and positive predictive value of MRI (both 93%) were still superior to values reported in previous Doppler studies.

The main advantage of MRI over Doppler is that MRI directly estimates hematocrit to detect anemia, since it utilizes the physical properties of blood, while MCA-PSV Doppler measures fetal circulatory consequences (i.e. lower viscosity) and adaptations (i.e. increased cardiac output) of fetal anemia. Fetal hemodynamic responses to anemia are likely to be variable, at least to some extent, and non-linear, while the MRI approach measures hematocrit across the full range. Recent studies have been exploring the potentials of combining MCA-PSV Doppler with other ultrasound measurements to improve the accuracy of ultrasound measures of fetal anemia, such as cardiofemoral index and descending aorta velocity.[110,111] However, these measurements, similar to MCA-PSV Doppler, are likely to be less reliable compared to the direct estimation of hematocrit level using MRI for the same reasons.

An alternative approach to deciding when to undertake repeat transfusions in anemic fetuses is to use an estimated rate of decline of hemoglobin concentration or hematocrit post-IUT in combination with the post-IUT hematocrit or hemoglobin level (Table 7). Comparing four different formulas (Table 7, Formula A-D) derived from their respective empirical data and the MCA-PSV Doppler measurements, the study by Ghesquière *et al* concluded that the use of such

formulas has poor specificity, particularly after the first IUT, and poor positive predictive value after the second IUT.[112] In addition, the rate of hematocrit decline post-transfusion differs significantly depending on the presence of hydrops.[109] However, Dodd *et al* showed that the use of an expected decline rate of hemoglobin or hematocrit post-transfusion is comparable to MCA-PSV Doppler for timing the following transfusions in 71 participants affected by RBC alloimmunization.[46] Other outcomes examined in the study included the newborn cord blood hemoglobin level and neonatal and/or maternal adverse outcome or complications due to alloimmunization or procedure. Despite the promising results, this method has only been validated in hemolytic fetal anemia, while MRI estimates of hematocrit is equally accurate in the setting of other causes of fetal anemia, allowing for broader application.

MCA-PSV Doppler alone cannot detect polycythemia in the MCDA twins in cases of TAPS.[113] Although the difference between MCA-PSV measures of the cotwins could be a better indicator of TAPS, the absolute MCA-PSV values of polycythemic fetuses are not always < 1 multiples of the median. In addition, the exact cut-off for MCA-PSV in polycythemia is still debatable.[33] The identification of polycythemia in these MCDA twin pregnancies is crucial as the transfusion of blood to the anemic cotwin could lead to aggravation of the condition and even intrauterine fetal death of the polycythemic twin. However, by directly estimating the hematocrit, we have shown that MRI could detect the absolute hematocrit level of both twins and the difference in hematocrit between the twins, and thus could become a better tool to diagnose inter-fetal blood transfusion in MCDA twins.

Table 6. Summary of results from studies using Doppler middle cerebral artery peak systolic velocity (MCA-PSV) to detect fetal anemia.

Study	GA (weeks)	Hb Reference for anemia	Sensitivity (%)	Specificity (%)	Negative PV (%)	Positive PV (%)
Mari *et al.*[3]	18 – 40	< 0.65 MoM	100	88	100	65
Zimmerman *et al.*[51]	16 – 35	< 0.65 MoM	88	87	98	53
Oepkes *et al.*[17]	17 - 38	> 5 SDs	88	82	89	80

Cut-off for MCA-PSV Doppler: 1.5 multiples of the median (MoM). Hb, hemoglobin; GA, gestational age; PV, predictive value.

Table 7. Summary of expected decrease rate of hemoglobin (Hb) or hematocrit (Hct) after intrauterine blood transfusions (IUT).

		Decreased rate between (g/dL/day or %)		
Formula	Use Hb or Hct	IUT 1 and 2	IUT 2 and 3	Reference
A	Hb	0.3	0.3	Nicolaides *et al*[114]
B	Hb	0.4	0.3	Scheier *et al*[8]
C	Hb	0.4	0.34	Garabedian *et al*[115]
D	Hb	0.45	0.35	Friszer *et al*[7]
E	Hct	1.2	0.96	Lobato and Sonici[109]

Table reproduced from Ghesquière *et al.* 2017.[112]

5.3 Limitations

5.3.1 Potential Causes of Inaccuracy

Inaccuracy in fetal hematocrit estimation by MRI could be introduced due to the small size of fetal vessels, as discussed in Section 5.1. Although we have shown that MRI is able to estimate fetal hematocrit with high accuracy compared to fetal blood sampling, larger differences between the two measurements still occur in some cases (maximum difference of 16%). MRI scans in fetuses at later gestations or in cases in which the blood vessels are dilated (as in severe anemia) are less likely to be affected by this limitation.

In addition, the selection of the region of interest during post processing could be another source of error, especially when the vessel of interest is small. Inclusion of the surrounding tissue would result in an underestimation of T_1 and thus overestimate hematocrit. The longitudinal relaxation of fetal tissues is usually shorter than that of blood (i.e. lower T_1).[87] This could partially explain why some of the MRI estimates of hematocrit were higher than the fetal blood sampling measurements. However, in our study, MRI tended to underestimate hematocrit by 3% overall, thus this is unlikely to be a major source of error.

Error also occurs in the process of curve fitting of the individual image signals from T_1 and T_2 mapping. The fitting error, or root-mean-square-deviation (RMSD) shown on Figure 20, indicates how accurate the predicted values from the model are compared to the measured values, which is related to the accuracy of the T_1 and T_2 measurements. Lower RMSD are generally signs of better fitting and thus higher accuracy. For the T_2 measurements in this study, the RMSD ranged from 2.6 - 22.4%, with an average of 9.5%. The average RMSD of T_1 measurements was higher (15%), most of which fell within the range of 6 - 24%. However, the RMSD of one T_1 measurement was 50.5%.

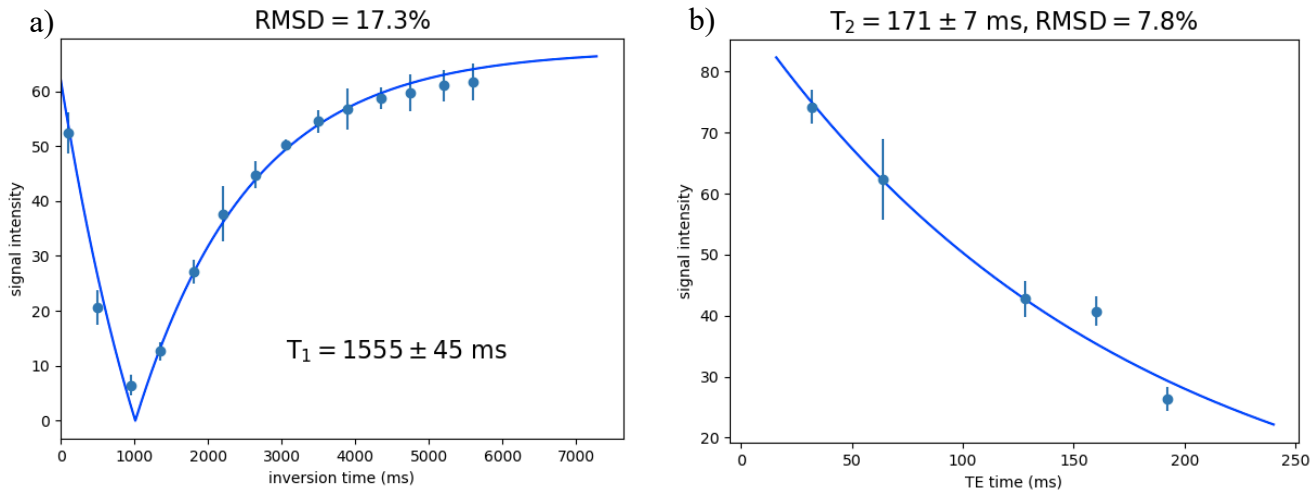

Figure 20. Examples of T_1 and T_2 curve-fitting.

a) T_1 recovery curve with RMSD of 17.3% from 14 data points. b) T_2 decay curve with RMSD of 7.8% from 5 data points. RMSD: root-mean-square-deviation.

5.3.2 Sample Size

The small sample size is a limitation of this study. This resulted from two factors that were not expected at the beginning of the study. Firstly, fetal anemia is a relatively rare condition. Despite being one of the most important sites for intrauterine blood transfusion in Canada, the actual number of transfusions performed at Mount Sinai Hospital during our study was not as large as we initially estimated based on prior years. In addition, some potential patients were missed because they required immediate treatment due to massive fetal-maternal hemorrhage or bleeding or were admitted outside of regular working hours when no staff was available to perform the MRI scan. As suggested by Dodd *et al*, the involvement of multiple centers in studying rare conditions or diseases could greatly shorten the duration of the study while maintaining strong statistical power.[46]

The availability of our MRI scanner was another factor that hampered the recruitment rate. The identification and consent of our potential participants generally occurred after their arrival at Mount Sinai Hospital, which was frequently organized on an emergent basis. The MRI appointment was thus scheduled after confirmation of the need for transfusion. While we made every effort to add these short scans to our MRI schedule at short notice, inevitably, there were

occasions when the scanner was unavailable during the short time window available to undertake the study. Collectively, these factors increased the difficulty of coordinating the MRI and blood transfusion between the two hospitals. We believe that the installation of a research MRI scanner at Mount Sinai Hospital will greatly improve the efficiency of scheduling and thus recruitment for future studies.

6 Conclusions and Future Directions

6.1 Conclusion

In conclusion, we describe our preliminary experience using MRI for estimating fetal hematocrit in the second and third trimesters in suspected fetal anemia. We found the technique to be well tolerated by patients and easily performed using standard 1.5 Tesla MRI equipment. Our analyses indicate that MRI is an excellent non-invasive tool to confidently exclude fetal anemia, especially later in the third trimester and following prior fetal blood transfusions, thereby overcoming an important limitation of MCA-PSV Doppler examinations in this context. Fetal MRI could therefore be a useful adjunct to Doppler ultrasound to help avoid unnecessary fetal blood sampling, with its attendant perinatal risks. However, the uptake of this method may be hampered by the cost and limited access to MRI. We therefore propose this method could be used in combination with MCA Doppler as a way to confirm or exclude anemia when there is uncertainty.

6.2 Future Directions

6.2.1 Applicability of T_1 and T_2 Mapping Sequences

Special referral centres that perform fetal blood transfusions usually have MRI scanners supplied by various manufacturers. Our current approach has only been validated on one of these vendors[101], and further technical development work would likely be necessary to allow for this approach on MRI systems provided by other vendors. The calculator used for estimating hematocrit and oxygen saturation based on relaxometry measurements is available through the SickKids website for both adult and fetal calibrations for 1.5T and 3T MR field strengths. In addition, if other centers were interested to adopt this approach in future, courses or training on the imaging and post-processing techniques would provide the MRI users with necessary expertise to analyze and interpret their results.

6.2.2 Understanding Hemodynamic Consequences of Fetal Anemia

Our understanding of the effects of anemia on fetal hemodynamics and metabolism are currently largely based on animal studies that employ acute isovolumic exchange transfusion to create an anemic model. Wolf *et al* have developed a model of fetal hemolytic anemia using direct intravascular injection of RBC-specific IgG antibodies into fetal sheep.[116] This sheep model exhibited a reduced fetal hematocrit and increased reticulocytes count, similar to those observed in anemic human fetuses. However, important differences exist between human and sheep physiology, including significantly lower hematocrit in normal fetal sheep compared with humans.[117] Direct measurements of fetal hemodynamics and oxygenation in human fetuses could therefore be helpful in terms of improving our understanding of the fetal circulatory physiology under anemic conditions. Previous work by our group has included the use of T_2 mapping and vessel blood flow measurements in normal fetuses, growth restricted fetuses, and fetuses with congenital heart disease at 1.5T and 3T.[84,85] These studies examined the oxygen saturation and blood flow in the major fetal vessels, including the main pulmonary artery, ascending and descending aorta, superior vena cava, ductus arteriosus and umbilical vein to estimate fetal oxygen delivery and consumption, and thus oxygen extraction fraction in these cohorts. While our *in vitro* validation study of T_1 and T_2 mapping on cord blood was not yet available when these studies were conducted, we assumed a normal hematocrit level and used the adult blood calibration to relate T_2 to oxygen saturation.[84–86] With the introduction of T_1 mapping and fetal calibration, the accuracy of our hemodynamic assessment of fetal anemia and other fetal conditions affecting circulatory physiology will become more accurate, allowing for potential improvements in our understanding of fetal circulatory adaptations to anemia.

A number of studies have investigated the influence of IUT on short- and long-term outcomes, including neurodevelopment and cardiovascular function. Cardiac MRI using CINE imaging can be used to assess cardiac function and circulatory physiology in human neonates and children.[118,119] These techniques have also been applied successfully in fetal sheep under anesthesia.[120] However, improved fetal cardiac MRI techniques are under development to achieve informative images non-invasively while overcoming the problems associated with fetal motion and the lack of cardiac gating.[121,122] MRI could therefore be used to examine cardiac function in anemic fetal patients before and after IUT to investigate the cardiovascular impact of anemia and IUT. Impaired placental and fetal hemodynamics are known to predispose to a risk

of subsequent neurodevelopmental impairment.[123] The combination of fetal and neonatal circulatory and neurodevelopment assessments possible with fetal and neonatal cardiovascular and brain MRI could provide us with a clearer understanding of the risks and benefits of treatments for patients with fetal anemia.

References

1. Papantoniou N, Sifakis S, Antsaklis A. Therapeutic management of fetal anemia: review of standard practice and alternative treatment options. J Perinat Med [Internet] 2013;41(1):71–82. Available from: https://www.degruyter.com/view/j/jpme.2013.41.issue-1/jpm-2012-0093/jpm-2012-0093.xml
2. Mari G, Norton ME, Stone J, et al. Society for Maternal-Fetal Medicine (SMFM) Clinical Guideline #8: The fetus at risk for anemia–diagnosis and management. Am J Obstet Gynecol [Internet] 2015;212(6):697–710. Available from: https://linkinghub.elsevier.com/retrieve/pii/S0002937815002033
3. Mari G, Deter RL, Carpenter RL, et al. Noninvasive Diagnosis by Doppler Ultrasonography of Fetal Anemia Due to Maternal Red-Cell Alloimmunization. N Engl J Med [Internet] 2000;342(1):9–14. Available from: http://www.nejm.org/doi/abs/10.1056/NEJM200001063420102
4. Berry SM, Stone J, Norton ME, Johnson D, Berghella V, Society for Maternal-Fetal Medicine. Fetal blood sampling. Am J Obstet Gynecol [Internet] 2013;209(3):170–80. Available from: http://dx.doi.org/10.1016/j.ajog.2013.07.014
5. Detti L, Oz U, Guney I, Ferguson JE, Bahado-Singh RO, Mari G. Doppler ultrasound velocimetry for timing the second intrauterine transfusion in fetuses with anemia from red cell alloimmunization. Am J Obstet Gynecol 2001;185(5):1048–51.
6. Mari G, Zimmermann R, Moise KJ, Deter RL. Correlation between middle cerebral artery peak systolic velocity and fetal hemoglobin after 2 previous intrauterine transfusions. Am J Obstet Gynecol [Internet] 2005;193(3):1117–20. Available from: https://linkinghub.elsevier.com/retrieve/pii/S0002937805009816
7. Friszer S, Maisonneuve E, Macé G, et al. Determination of optimal timing of serial in-utero transfusions in red-cell alloimmunization. Ultrasound Obstet Gynecol [Internet] 2015;46(5):600–5. Available from: http://doi.wiley.com/10.1002/uog.14772
8. Scheier M, Hernandez-Andrade E, Fonseca EB, Nicolaides KH. Prediction of severe fetal anemia in red blood cell alloimmunization after previous intrauterine transfusions. Am J Obstet Gynecol [Internet] 2006;195(6):1550–6. Available from: https://linkinghub.elsevier.com/retrieve/pii/S0002937806004479
9. Martinez-Portilla RJ, Lopez-Felix J, Hawkins-Villareal A, et al. Performance of middle cerebral artery peak systolic velocity for the prediction of fetal anemia in untransfused and transfused fetuses: a diagnostic test accuracy meta-analysis. Ultrasound Obstet Gynecol [Internet] 2019;uog.20273. Available from: https://onlinelibrary.wiley.com/doi/abs/10.1002/uog.20273
10. Jopling J, Henry E, Wiedmeier SE, Christensen RD. Reference Ranges for Hematocrit and Blood Hemoglobin Concentration During the Neonatal Period: Data From a Multihospital Health Care System. Pediatrics 2009;123(2).
11. Abbasi N, Johnson JA, Ryan G. Fetal anemia. Ultrasound Obstet Gynecol 2017;50(2):145–53.
12. Fan FC, Chen RY, Schuessler GB, Chien S. Effects of hematocrit variations on regional hemodynamics and oxygen transport in the dog. Am J Physiol Circ Physiol 1980;238(4):H545–52.
13. Van Ameringen MR, Fouron JC, Bard H, Le Guennec JC, Prosmanne J. Oxygenation in Anemic Newborn Lambs with High or Low Oxygen Affinity Red Cells. Pediatr Res

[Internet] 1981;15(12):1500–3. Available from: http://www.nature.com/doifinder/10.1203/00006450-198112000-00009
14. Oberhoffer R, Grab D, Keckstein J, Högel J, Terinde R, Lang D. Cardiac changes in fetuses secondary to immune hemolytic anemia and their relation to hemoglobin and catecholamine concentrations in fetal blood. Ultrasound Obstet Gynecol [Internet] 1999;13(6):396–400. Available from: http://doi.wiley.com/10.1046/j.1469-0705.1999.13060396.x
15. Bigras JL, Suda K, Dahdah NS, Fouron JC. Cardiovascular evaluation of fetal anemia due to alloimmunization. Fetal Diagn Ther 2008;24(3):197–202.
16. Mesogitis S, Daskalakis G, Pilalis A, Papantoniou N, Antsaklis A. Fetal Intravascular Transfusion for Hydropic Disease due to Rhesus Isoimmunization. Fetal Diagn Ther [Internet] 2005;20(5):431–6. Available from: https://www.karger.com/Article/FullText/86826
17. Oepkes D, Seaward PG, Vandenbussche FPHA, et al. Doppler Ultrasonography versus Amniocentesis to Predict Fetal Anemia. Obstet Gynecol Surv [Internet] 2006;61(11):703–4. Available from: https://insights.ovid.com/crossref?an=00006254-200611000-00011
18. Jonker SS, Giraud MK, Giraud GD, et al. Cardiomyocyte enlargement, proliferation and maturation during chronic fetal anaemia in sheep. Exp Physiol [Internet] 2010;95(1):131–9. Available from: http://doi.wiley.com/10.1113/expphysiol.2009.049379
19. Bowman JM. Antenatal Suppression of Rh Alloimmunization. Clin Obstet Gynecol 1991;34(2):296–303.
20. Dukler D, Oepkes D, Seaward G, Windrim R, Ryan G. Noninvasive tests to predict fetal anemia: A study comparing Doppler and ultrasound parameters. Am J Obstet Gynecol 2003;188(5):1310–4.
21. Weiner CP, Widness JA. Decreased fetal erythropoiesis and hemolysis in Kell hemolytic anemia. Am J Obstet Gynecol 1996;174(2):547–51.
22. Nicolaides KH, Clewell WH, Mibashan RS, Soothill PW, Rodeck CH, Campbell S. Fetal Haemoglobin Measurement in the Assessment of Red Cell Isoimmunisation. Lancet 1988;331(8594):1073–5.
23. Moise KJ, Argoti PS. Management and prevention of red cell alloimmunization in pregnancy: a systematic review. Obstet Gynecol [Internet] 2012;120(5):1132–9. Available from: http://www.ncbi.nlm.nih.gov/pubmed/23090532
24. Zwingerman R, Jain V, Hannon J, Zwingerman N, Clarke G. Alloimmune Red Blood Cell Antibodies: Prevalence Pathogenicity in a Canadian Prenatal Population. J Obstet Gynaecol Canada 2015;37(9):784–90.
25. Snowise S, Johnson A. Immune Hydrops Fetalis [Internet]. Second Edi. Elsevier Inc.; 2017. Available from: http://dx.doi.org/10.1016/B978-0-323-44548-1.00123-6
26. Dean L. Chapter 4 . Hemolytic disease of the newborn. In: Blood Groups and Red Cell Antigens [Internet]. Bethesda (MD): National Center for Biotechnology Information (US); 2005.
27. Bowman JM, Pollock JM, Penston LE. Fetomaternal Transplacental Hemorrhage during Pregnancy and after Delivery. Vox Sang [Internet] 1986;51(2):117–21. Available from: http://www.embase.com/search/results?subaction=viewrecord&from=export&id=L16046151%5Cnhttp://sfx.library.uu.nl/utrecht?sid=EMBASE&issn=00429007&id=doi:&atitle=Fetomaternal+transplacental+hemorrhage+during+pregnancy+and+after+delivery&stitle=VOX+SANG.&titl
28. Brennand J, Cameron A. Fetal anaemia: diagnosis and management. Best Pract Res Clin Obstet Gynaecol [Internet] 2008;22(1):15–29. Available from:

https://linkinghub.elsevier.com/retrieve/pii/S1521693407001381
29. Illanes S, Peter S. Management of red cell allommunisation in pregnancy: the non-invasive monitoring of the disease. Prenat Diagn 2010;30(1):668–73.
30. Heegaard ED, Brown KE. Human Parvovirus B19. Clin Microbiol Rev [Internet] 2002;15(3):485–505. Available from: http://cmr.asm.org/cgi/doi/10.1128/CMR.15.3.485-505.2002
31. Crane J, Mundle W, Boucoiran I, et al. Parvovirus B19 Infection in Pregnancy. J Obstet Gynaecol Canada [Internet] 2014;36(12):1107–16. Available from: http://dx.doi.org/10.1016/S1701-2163(15)30390-X
32. Chui DHK, Fucharoen S, Chan V. Hemoglobin H disease: not necessarily a benign disorder. Blood [Internet] 2003;101(3):791–800. Available from: http://www.bloodjournal.org/cgi/doi/10.1182/blood-2002-07-1975
33. Slaghekke F, Kist WJ, Oepkes D, et al. Twin anemia-polycythemia sequence: Diagnostic criteria, classification, perinatal management and outcome. Fetal Diagn Ther 2010;27(4):181–90.
34. Lopriore E, Middeldorp JM, Oepkes D, Kanhai HH, Walther FJ, Vandenbussche FPHA. Twin Anemia-Polycythemia Sequence in Two Monochorionic Twin Pairs Without Oligo-Polyhydramnios Sequence. Placenta 2007;28(1):47–51.
35. Nicholas LD, Fischbein RL, Bhamidipalli SS. Twin anemia-polycythemia sequence and routine monitoring practices amongst maternal-fetal medicine specialists in the United States: An initial investigation. J Perinat Med 2019;47(4):388–92.
36. Lopriore E, Slaghekke F, Oepkes D, Middeldorp JM, Vandenbussche FP, Walther FJ. Clinical outcome in neonates with twin anemia-polycythemia sequence. Am J Obstet Gynecol [Internet] 2010;203(1):54.e1-54.e5. Available from: http://dx.doi.org/10.1016/j.ajog.2010.02.032
37. Haak MC, Oosterhof H, Mouw RJ, Oepkes D, Vandenbussche FPHA. Pathophysiology and treatment of fetal anemia due to placental chorioangioma. Ultrasound Obstet Gynecol [Internet] 1999;14(1):68–70. Available from: http://doi.wiley.com/10.1046/j.1469-0705.1999.14010068.x
38. Pott Bärtsch EM, Paek BW, Yoshizawa J, et al. Giant Fetal Hepatic Hemangioma. Fetal Diagn Ther 2003;18(1):59–64.
39. Fan M, Skupski DW. Placental chorioangioma: Literature review. J Perinat Med 2014;42(3):273–9.
40. Sankaran VG, Orkin SH. The switch from fetal to adult hemoglobin. Cold Spring Harb Perspect Med 2013;3(1):1–14.
41. Rodeck CH, Campbell S. UMBILICAL-CORD INSERTION AS SOURCE OF PURE FETAL BLOOD FOR PRENATAL DIAGNOSIS. Lancet [Internet] 1979;313(8128):1244–5. Available from: https://linkinghub.elsevier.com/retrieve/pii/S0140673679919287
42. Liley AW. Liquor amnii analysis in the management of the pregnancy complicated by rhesus sensitization. Am J Obstet Gynecol [Internet] 1961;82(6):1359–70. Available from: http://dx.doi.org/10.1016/S0002-9378(16)36265-2
43. Queenan JT, Tomai TP, Ural SH, King JC. Deviation in amniotic fluid optical density at a wavelength of 450 nm in Rh-immunized pregnancies from 14 to 40 weeks' gestation: A proposal for clinical management. Am J Obstet Gynecol [Internet] 1993;168(5):1370–6. Available from: http://dx.doi.org/10.1016/S0002-9378(11)90767-4
44. Spinnato J, Clark AL, Ralston KK, Greenwell ER, Goldsmith LJ. Hemolytic disease of the fetus: a comparison of the Queenan and extended Liley methods. Obstet Gynecol

[Internet] 1998;92(3):441–5. Available from: http://linkinghub.elsevier.com/retrieve/pii/S0029784498001793
45. Scott F, Chan FY. Assessment of the clinical usefulness of the “Queenan” chart versus the “Liley” chart in predicting severity of rhesus iso-immunization. Prenat Diagn 1998;18(11):1143–8.
46. Dodd JM, Andersen C, Dickinson JE, et al. Fetal middle cerebral artery Doppler to time intrauterine transfusion in red-cell alloimmunization: a randomized trial. Ultrasound Obstet Gynecol [Internet] 2018;51(3):306–12. Available from: http://doi.wiley.com/10.1002/uog.18807
47. Nicolaides KH, Fontanarosa M, Gabbe SG, Rodeck CH. Failure of ultrasonographic parameters to predict the severity of fetal anemia in rhesus isoimmunization. Am J Obstet Gynecol 1988;158(4):920–6.
48. Teixeira JMA, Duncan K, Letsky E, Fisk NM. Middle cerebral artery peak systolic velocity in the prediction of fetal anemia. Ultrasound Obstet Gynecol [Internet] 2000;15(3):205–8. Available from: http://doi.wiley.com/10.1046/j.1469-0705.2000.00070.x
49. Kirkinen P, Jouppila P, Eik-Nes S. UMBILICAL VENOUS FLOW AS INDICATOR OF FETAL ANAEMIA. Lancet [Internet] 1981;317(8227):1004–5. Available from: https://linkinghub.elsevier.com/retrieve/pii/S014067368191775X
50. Nicolaides KH, Bilardo CM, Campbell S. Prediction of fetal anemia by measurement of the mean blood velocity in the fetal aorta. Am J Obstet Gynecol [Internet] 1990;162(1):209–12. Available from: https://linkinghub.elsevier.com/retrieve/pii/000293789090852X
51. Zimmermann R, Durig P, Carpenter RJ, Mari G. Longitudinal measurement of peak systolic velocity in the fetal middle cerebral artery for monitoring pregnancies complicated by red cell alloimmunisation: a prospective multicentre trial with intention-to-treat. BJOG An Int J Obstet Gynaecol [Internet] 2002;109(7):746–52. Available from: http://doi.wiley.com/10.1111/j.1471-0528.2002.01314.x
52. Leung WC, Oepkes D, Seaward G, Ryan G. Serial sonographic findings of four fetuses with homozygous alpha-thalassemia-1 from 21 weeks onwards. Ultrasound Obstet Gynecol 2002;19(1):56–9.
53. Cosmi E, Mari G, Chiaie LD, et al. Noninvasive diagnosis by Doppler ultrasonography of fetal anemia resulting from parvovirus infection. Am J Obstet Gynecol 2002;187(5):1290–3.
54. Van Dongen H, Klumper FJCM, Sikkel E, Vandenbussche FPHA, Oepkes D. Non-invasive tests to predict fetal anemia in Kell-alloimmunized pregnancies. Ultrasound Obstet Gynecol 2005;25(4):341–5.
55. Picklesimer AH, Oepkes D, Moise KJ, et al. Determinants of the middle cerebral artery peak systolic velocity in the human fetus. Am J Obstet Gynecol 2007;197(5):526.e1-526.e4.
56. Pretlove SJ, Fox CE, Khan KS, Kilby MD. Noninvasive methods of detecting fetal anaemia : a systematic review and meta-analysis. BJOG An Int J Obstet Gynaecol 2009;116(12):1558–67.
57. Vaughan JI, Manning M, Warwick RM, Letsky EA, Murray NA, Roberts IAG. Inhibition of Erythroid Progenitor Cells by Anti-Kell Antibodies in Fetal Alloimmune Anemia. N Engl J Med [Internet] 1998;338(12):798–803. Available from: https://linkinghub.elsevier.com/retrieve/pii/S0140673677925600
58. Tongprasert F, Srisupundit K, Luewan S, Traisrisilp K, Jatavan P, Tongsong T. The best

cutoff value of middle cerebral artery peak systolic velocity for the diagnosis of fetal homozygous alpha thalassemia-1 disease. Prenat Diagn 2019;39(3):232–7.
59. Veujoz M, Sananès N, Severac F, et al. Evaluation of prenatal and postnatal diagnostic criteria for twin anemia-polycythemia sequence. Prenat Diagn 2015;35(3):281–8.
60. Slaghekke F, Pasman S, Veujoz M, et al. Middle cerebral artery peak systolic velocity to predict fetal hemoglobin levels in twin anemia-polycythemia sequence. Ultrasound Obstet Gynecol 2015;46(4):432–6.
61. Maisonneuve E, Jayot A, Friszer S, et al. Accuracy of Middle Cerebral Artery Doppler Assessment between 34 and 37 Weeks in Fetuses with Red Cell Alloimmunization. Fetal Diagn Ther 2017;42(3):225–31.
62. Yoder BA, Gordon MC, Barth WH. Late-Preterm Birth. Obstet Gynecol 2010;111(4):814–22.
63. Zwiers C, van Kamp I, Oepkes D, Lopriore E. Intrauterine transfusion and non-invasive treatment options for hemolytic disease of the fetus and newborn – review on current management and outcome. Expert Rev Hematol [Internet] 2017;10(4):337–44. Available from: https://doi.org/10.1080/17474086.2017.1305265
64. Palmeira P, Quinello C, Silveira-Lessa AL, Zago CA, Carneiro-Sampaio M. IgG Placental Transfer in Healthy and Pathological Pregnancies. Clin Dev Immunol [Internet] 2012;2012:1–13. Available from: http://www.hindawi.com/journals/jir/2012/985646/
65. Liley A. Intrauterine Transfusion of Foetus in Haemolytic Disease. Br Med J 1963;2:1107–9.
66. Rodeck CH, Holman CA, Karnicki J, Kemp JR, Whitmore DN, Austin MA. Direct Intravascular Fetal Blood Transfusion By Fetoscopy in Severe Rhesus Isoimmunisation. Lancet 1981;317(8221):625–7.
67. Bang J, Bock JE, Trolle D. Ultrasound-guided fetal intravenous transfusion for severe rhesus haemolytic disease. Br Med J (Clin Res Ed) 1982;284(6313):373–4.
68. Zwiers C, Lindenburg ITM, Klumper FJ, de Haas M, Oepkes D, Van Kamp IL. Complications of intrauterine intravascular blood transfusion: lessons learned after 1678 procedures. Ultrasound Obstet Gynecol 2017;50(2):180–6.
69. Moise KJ. Management of rhesus alloimmunization in pregnancy. Obstet Gynecol 2008;112(1):164–76.
70. Kingdom JCP, Ryan G, Whittle MJ, et al. Atrial natriuretic peptide: A vasodilator of the fetoplacental circulation? Am J Obstet Gynecol [Internet] 1991;165(4):791–800. Available from: https://linkinghub.elsevier.com/retrieve/pii/000293789190419R
71. Radunovic N, Lockwood CJ, Alvarez M, Plecas D, Chitkara U, Berkowitz RL. The Severely Anemic and Hydropic Isoimmune Fetus. Obstet Gynecol [Internet] 1992;79(3):390–3. Available from: https://insights.ovid.com/crossref?an=00006250-199203000-00013
72. Eckmann DM, Bowers S, Stecker M, Cheung AT. Hematocrit, volume expander, temperature, and shear rate effects on blood viscosity. Anesth Analg 2000;91(3):539–45.
73. Welch R, Rampling MW, Anwar A, Talbert DG, Rodeck CH. Changes in hemorheology with fetal intravascular transfusion. Am J Obstet Gynecol 1994;170(3):726–32.
74. Lindenburg ITM, Van Kamp IL, Oepkes D. Intrauterine blood transfusion: Current indications and associated risks. Fetal Diagn Ther 2014;36(4):263–71.
75. Van Kamp IL, Klumper FJCM, Bakkum RSLA, et al. The severity of immune fetal hydrops is predictive of fetal outcome after intrauterine treatment. Am J Obstet Gynecol 2001;185(3):668–73.
76. Schumacher B, Moise Jr K. Fetal transfusion for red blood cell alloimmunization in

pregnancy. Obstet Gynecol [Internet] 1996;88(1):137–50. Available from: http://linkinghub.elsevier.com/retrieve/pii/0029784496001135
77. Lindenburg ITM, van Klink JM, Smits-Wintjens VEHJ, van Kamp IL, Oepkes D, Lopriore E. Long-term neurodevelopmental and cardiovascular outcome after intrauterine transfusions for fetal anaemia: A review. Prenat Diagn 2013;33(9):815–22.
78. Lindenburg IT, Smits-Wintjens VE, Van Klink JM, et al. Long-term neurodevelopmental outcome after intrauterine transfusion for hemolytic disease of the fetus/newborn: The LOTUS study. Am J Obstet Gynecol [Internet] 2012;206(2):141.e1-141.e8. Available from: http://dx.doi.org/10.1016/j.ajog.2011.09.024
79. Harper DC, Swingle HM, Weiner CP, Bonthius DJ, Aylward GP, Widness JA. Long-term neurodevelopmental outcome and brain volume after treatment for hydrops fetalis by in utero intravascular transfusion. Am J Obstet Gynecol 2006;195(1):192–200.
80. Van Klink JMM, Koopman HM, Oepkes D, Walther FJ, Lopriore E. Long-term neurodevelopmental outcome after intrauterine transfusion for fetal anemia. Early Hum Dev [Internet] 2011;87(9):589–93. Available from: http://dx.doi.org/10.1016/j.earlhumdev.2011.07.003
81. Wallace AH, Dalziel SR, Cowan BR, Young AA, Thornburg KL, Harding JE. Long-term cardiovascular outcome following fetal anaemia and intrauterine transfusion: A cohort study. Arch Dis Child 2017;102(1):40–5.
82. van Kamp IL, Klumper FJCM, Oepkes D, et al. Complications of intrauterine intravascular transfusion for fetal anemia due to maternal red-cell alloimmunization. Am J Obstet Gynecol [Internet] 2005;192(1):171–7. Available from: https://linkinghub.elsevier.com/retrieve/pii/S0002937804006635
83. Saleem SN. Fetal MRI: An approach to practice: A review. J Adv Res [Internet] 2014;5(5):507–23. Available from: http://dx.doi.org/10.1016/j.jare.2013.06.001
84. Sun L, Macgowan C, Sled J, et al. Reduced Fetal Cerebral Oxygen Consumption is Associated With Smaller Brain Size in Fetuses With Congenital Heart Disease. Circulation 2015;131(15):1313–23.
85. Zhu MY, Milligan N, Keating S, et al. The hemodynamics of late-onset intrauterine growth restriction by MRI. Am J Obstet Gynecol 2016;214(3):367.e1-367.e17.
86. Portnoy S, Osmond M, Zhu MY, Seed M, Sled JG, Macgowan CK. Relaxation properties of human umbilical cord blood at 1.5 Tesla. Magn Reson Med 2017;77(4):1678–90.
87. McRobbie DW, Moore EA, Graves MJ, Prince MR. Getting in tune: resonance and relaxation [Internet]. In: MRI From Picture to Proton. Cambridge: Cambridge University Press; 2019. p. 137–66.Available from: https://www.cambridge.org/core/product/identifier/CBO9780511545405A074/type/book_part
88. Bloch F. Nuclear Induction. Phys Rev [Internet] 1946;70(7–8):460–74. Available from: https://link.aps.org/doi/10.1103/PhysRev.70.460
89. Carneiro AAO, Vilela GR, Araujo DB de, Baffa O. MRI relaxometry: methods and applications. Brazilian J Phys 2006;36(1a):1–7.
90. Taylor AJ, Salerno M, Dharmakumar R, Jerosch-Herold M. T1 Mapping. JACC Cardiovasc Imaging [Internet] 2016;9(1):67–81. Available from: https://linkinghub.elsevier.com/retrieve/pii/S1936878X15008670
91. Messroghli DR, Radjenovic A, Kozerke S, Higgins DM, Sivananthan MU, Ridgway JP. Modified look-locker inversion recovery (MOLLI) for high-resolution T 1 mapping of the heart. Magn Reson Med 2004;52(1):141–6.
92. Portnoy S. Fetal Magnetic Resonance Oximetry [Internet]. 2018;Available from:

http://hdl.handle.net/1807/91949
93. Wright GA, Hu BS, Macovski A. Estimating Oxygen Saturauon of Blood in Vivo with MR Imaging at 1.5 T. Jmri 1991;1:275–83.
94. Liu P, Chalak LF, Krishnamurthy LC, et al. T1 and T2 values of human neonatal blood at 3 Tesla: Dependence on hematocrit, oxygenation, and temperature. Magn Reson Med [Internet] 2016;75(4):1730–5. Available from: http://doi.wiley.com/10.1002/mrm.25775
95. Grgac K, Van Zijl PCM, Qin Q. Hematocrit and oxygenation dependence of blood 1H2O T1 at 7 tesla. Magn Reson Med 2013;70(4):1153–9.
96. Stefanovic B, Pike GB. Human whole-blood relaxometry at 1.5T: Assessment of diffusion and exchange models. Magn Reson Med 2004;52(4):716–23.
97. Portnoy S, Milligan N, Seed M, Sled JG, Macgowan CK. Human umbilical cord blood relaxation times and susceptibility at 3 T. Magn Reson Med 2018;79(6):3194–206.
98. Linderkamp O, Wu PY, Meiselman HJ. Geometry of neonatal and adult red blood cells. Pediatr Res 1983;17(4):250–3.
99. Reinhart WH, Danoff SJ, King RG, Chien S. Rheology of fetal and maternal blood. Pediatr Res 1985;19(1):147–53.
100. Barton TC. Water Permeability of the Fetal Erythrocyte. J Gen Physiol 2004;47(5):839–49.
101. Portnoy S, Seed M, Sled JG, Macgowan CK. Non-invasive evaluation of blood oxygen saturation and hematocrit from T1 and T2 relaxation times: In-vitro validation in fetal blood. Magn Reson Med 2017;78(6):2352–9.
102. Seed M, Macgowan CK. Fetal Cardiovascular MRI. Magnetom Flash 2014;66–72.
103. Stainsby JA, Wright GA. Partial volume effects on vascular T2 measurements. Magn Reson Med 1998;40(3):494–9.
104. Mari G, Adrignolo A, Abuhamad AZ, et al. Diagnosis of fetal anemia with Doppler ultrasound in the pregnancy complicated by maternal blood group immunization. Ultrasound Obstet. Gynecol. 1995;5(6):400–5.
105. Briggs C, Bain BJ. Basic Haematological Techniques [Internet]. In: Lewis M, editor. Dacie and Lewis Practical Haematology. Philadelphia, Pa.: Elsevier; 2017. p. 18–49.Available from: https://linkinghub.elsevier.com/retrieve/pii/B9780702066962000035
106. Jørgensen DS, Vejlstrup N, Rode L, et al. Magnetic Resonance Imaging: A New Tool to Optimize the Prediction of Fetal Anemia? Fetal Diagn Ther [Internet] 2019;7:1–9. Available from: https://www.karger.com/Article/FullText/494615
107. Estroff JA, Benacerraf BR. Fetal umbilical vein varix: sonographic appearance and postnatal outcome. J Ultrasound Med [Internet] 1992;11(3):69–73. Available from: http://doi.wiley.com/10.7863/jum.1992.11.3.69
108. Steiner LA, Gallagher PG. Erythrocyte Disorders in the Perinatal Period in Adverse Pregnancy Outcomes and the Fetus/Neonate. Semin Perinatol 2007;31(4):254–61.
109. Lobato G, Soncini CS. Fetal hematocrit decrease after repeated intravascular transfusions in alloimmunized pregnancies. Arch Gynecol Obstet [Internet] 2007;276(6):595–9. Available from: http://link.springer.com/10.1007/s00404-007-0382-9
110. Cabral ACV, Reis ZSN, Apocalypse IG, Osanan GC, Lage EM, Leite HV. Combined use of the cardiofemoral index and middle cerebral artery Doppler velocimetry for the prediction of fetal anemia. Int J Gynecol Obstet 2010;111(3):205–8.
111. Pares D, Chinen PA, Camano L, Moron AF, Torloni MR. Prediction of fetal anemia by Doppler of the middle cerebral artery and descending thoracic aorta. Arch Gynecol Obstet 2008;278(1):27–31.
112. Ghesquière L, Houfflin-Debarge V, Behal H, et al. Should optimal timing between two

intrauterine transfusions be based on estimated daily decrease of hemoglobin or on measurement of fetal middle cerebral artery peak systolic velocity? Transfusion [Internet] 2017;57(4):899–904. Available from: http://doi.wiley.com/10.1111/trf.13980
113. Fishel-Bartal M, Weisz B, Mazaki-Tovi S, et al. Can middle cerebral artery peak systolic velocity predict polycythemia in monochorionic–diamniotic twins? Evidence from a prospective cohort study. Ultrasound Obstet Gynecol [Internet] 2016;48(4):470–5. Available from: http://doi.wiley.com/10.1002/uog.15838
114. Nicolaides K, Soothill P, Rodeck C. Rh disease: intravascular fetal blood transfusion by cordocentesis. Fetal Diagnosis and [Internet] 1986;185–92. Available from: http://www.karger.com/Article/Abstract/262267
115. Garabedian C, Rakza T, Thomas D, et al. Neonatal outcome after fetal anemia managed by intrauterine transfusion. Eur J Pediatr 2015;174(11):1535–9.
116. Wolf RB, Moise Jr K, Brace RA. Antibody-induced anemia in fetal sheep: model for hemolytic disease of the fetus and newborn. J Soc Gynecol Investig [Internet] 2001;8(4):224–32. Available from: http://linkinghub.elsevier.com/retrieve/pii/S1071557601001071
117. Rudolph AM. Congenital Diseases of the Heart [Internet]. 3rd ed. Oxford, UK: Wiley-Blackwell; 2009. Available from: http://doi.wiley.com/10.1002/9781444311822
118. Seed M, F P van Amerom J, Yoo S-J, et al. Feasibility of quantification of the distribution of blood flow in the normal human fetal circulation using CMR: a cross-sectional study. J Cardiovasc Magn Reson [Internet] 2012;14(1):79. Available from: https://jcmr-online.biomedcentral.com/articles/10.1186/1532-429X-14-79
119. Lim JM, Kingdom T, Saini B, et al. Cerebral oxygen delivery is reduced in newborns with congenital heart disease. J Thorac Cardiovasc Surg [Internet] 2016;152(4):1095–103. Available from: http://dx.doi.org/10.1016/j.jtcvs.2016.05.027
120. Duan AQ, Darby J, Soo JY, et al. Feasibility of phase-contrast cine magnetic resonance imaging for measuring blood flow in the sheep fetus. Am Physiol Soc 2017;30(11):1662–81.
121. Roy CW, Seed M, Macgowan CK. Accelerated MRI of the fetal heart using compressed sensing and metric optimized gating. Magn Reson Med [Internet] 2017;77(6):2125–35. Available from: http://doi.wiley.com/10.1002/mrm.26290
122. Roy CW, Seed M, Kingdom JC, Macgowan CK. Motion compensated cine CMR of the fetal heart using radial undersampling and compressed sensing. J Cardiovasc Magn Reson 2017;19(1):1–14.
123. Peixoto AB, Tonni G, Júnior EA. Changes in biometry and cerebroplacental hemodynamics in fetuses with congenital heart diseases. J Thorac Dis 2016;8(10):E1282–6.

Appendices

Appendix I. Equations of T_1 and T_2 relaxation. Adapted from Portnoy *et al*.[92]

Equation 1:

$$M_Z(t) = M_0 + [M_Z(t=0) - M_0] \cdot e^{-t/T_1}$$

Equation 2:

$$M_{xy}(t) = M_{xy}(t=0) \cdot e^{-t/T_2}$$

Equation 3:

$$\mathrm{Hct} = \frac{R_1 - R_{1,plas}}{R_{1,ery,0} - R_{1,plas} + (1 - SaO2) \cdot r'_{1\ dHb}}$$

Appendix II. Intra- and inter-observer validation

Figure S1. Intra-observer agreement of MRI T_1 and T_2 measurements.

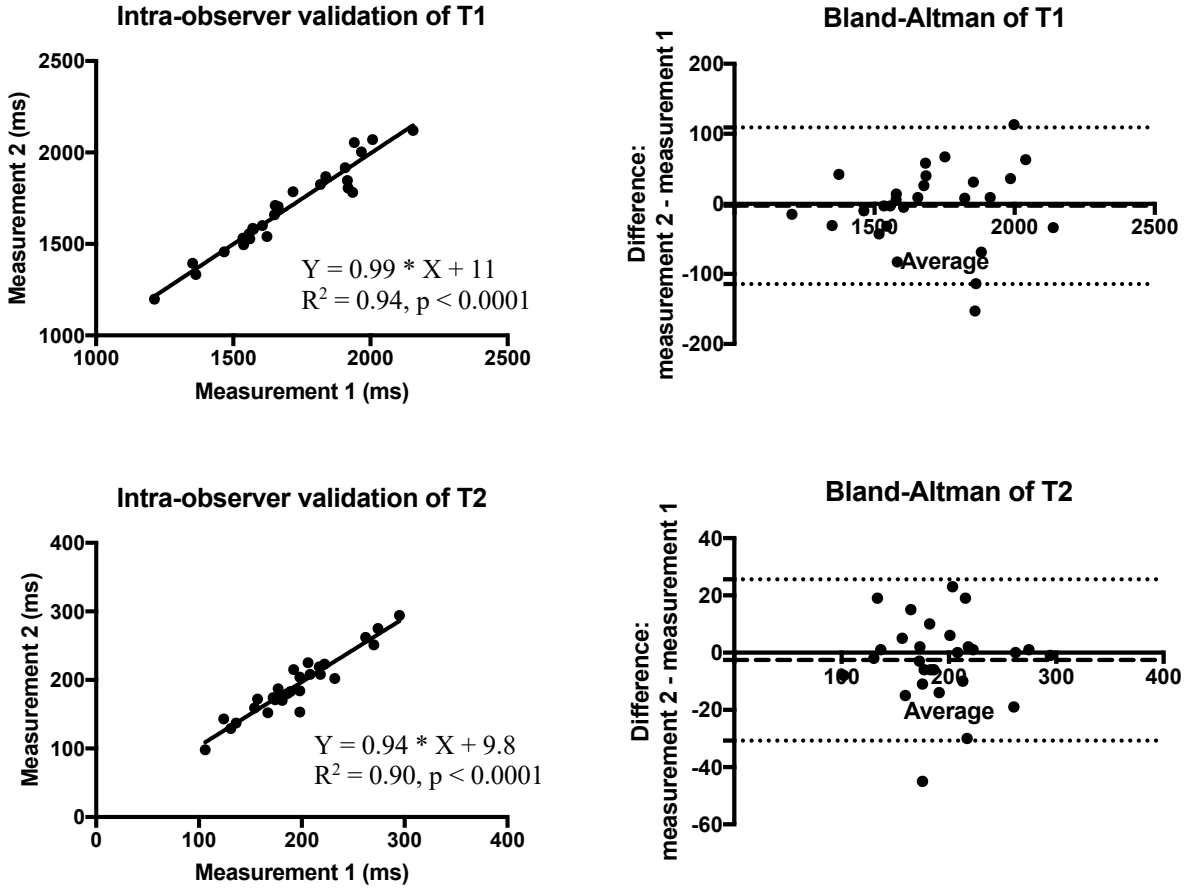

Figure S2. Inter-observer agreement of MRI T_1 and T_2 measurements.

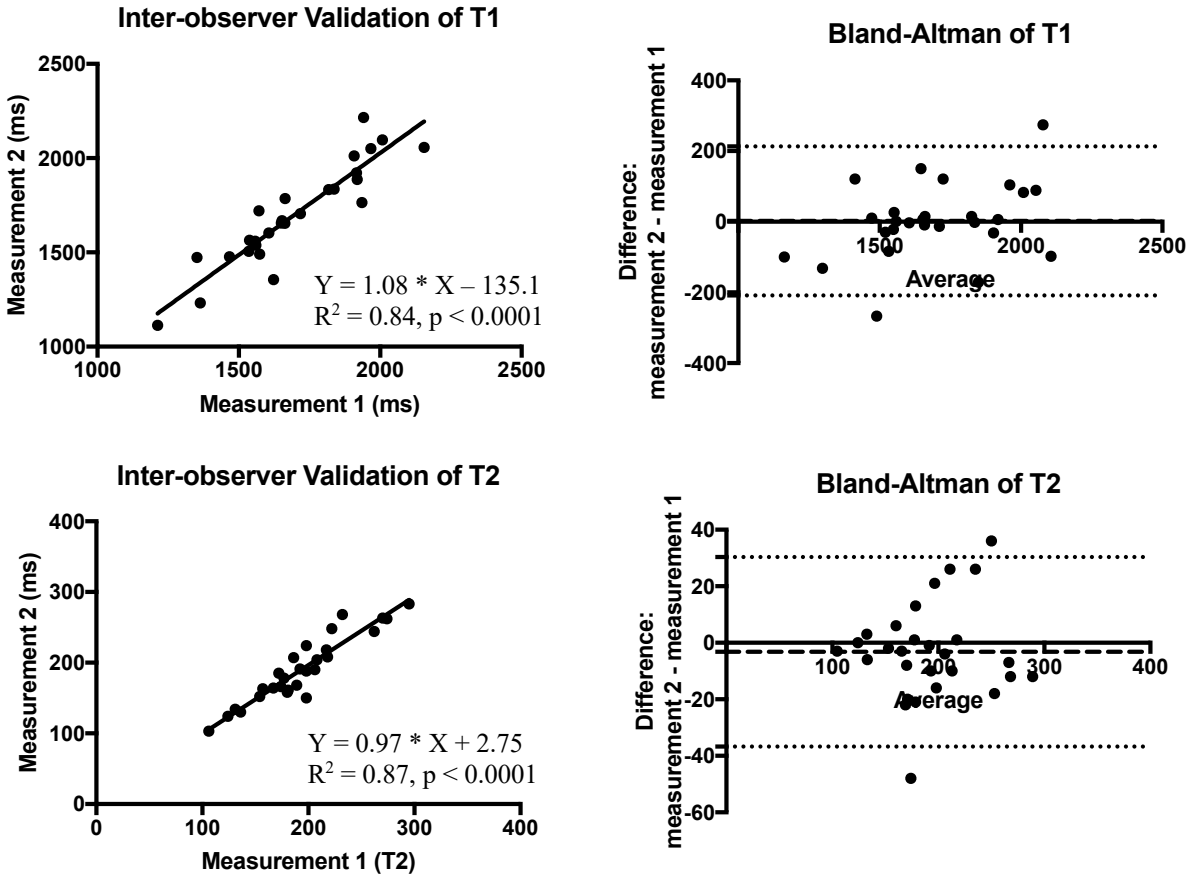

Appendix III. Contingency tables of MRI and Doppler measurement.

Table S1. Contingency table based on all MRI pre-transfusion measurements.

Diagnosis / MRI results	Moderate-to-severe anemia	Mild anemia or normal	Total
Test positive	10	1	11
Test negative	1	13	14
Total	11	14	25

Cut-off for moderate-to-severe anemia: 0.65 multiples of the median. Diagnosis was made based on laboratory hematocrit level from fetal blood sampling.

Table S2. Contingency table based on all Doppler pre-transfusion measurements.

Diagnosis / Doppler results	Moderate-to-severe anemia	Mild anemia or normal	Total
Test positive	10	4	14
Test negative	1	10	11
Total	11	14	25

Cut-off for moderate-to-severe anemia: 1.5 multiples of the median. Diagnosis was made based on laboratory hematocrit level from fetal blood sampling.

Copyright Acknowledgements

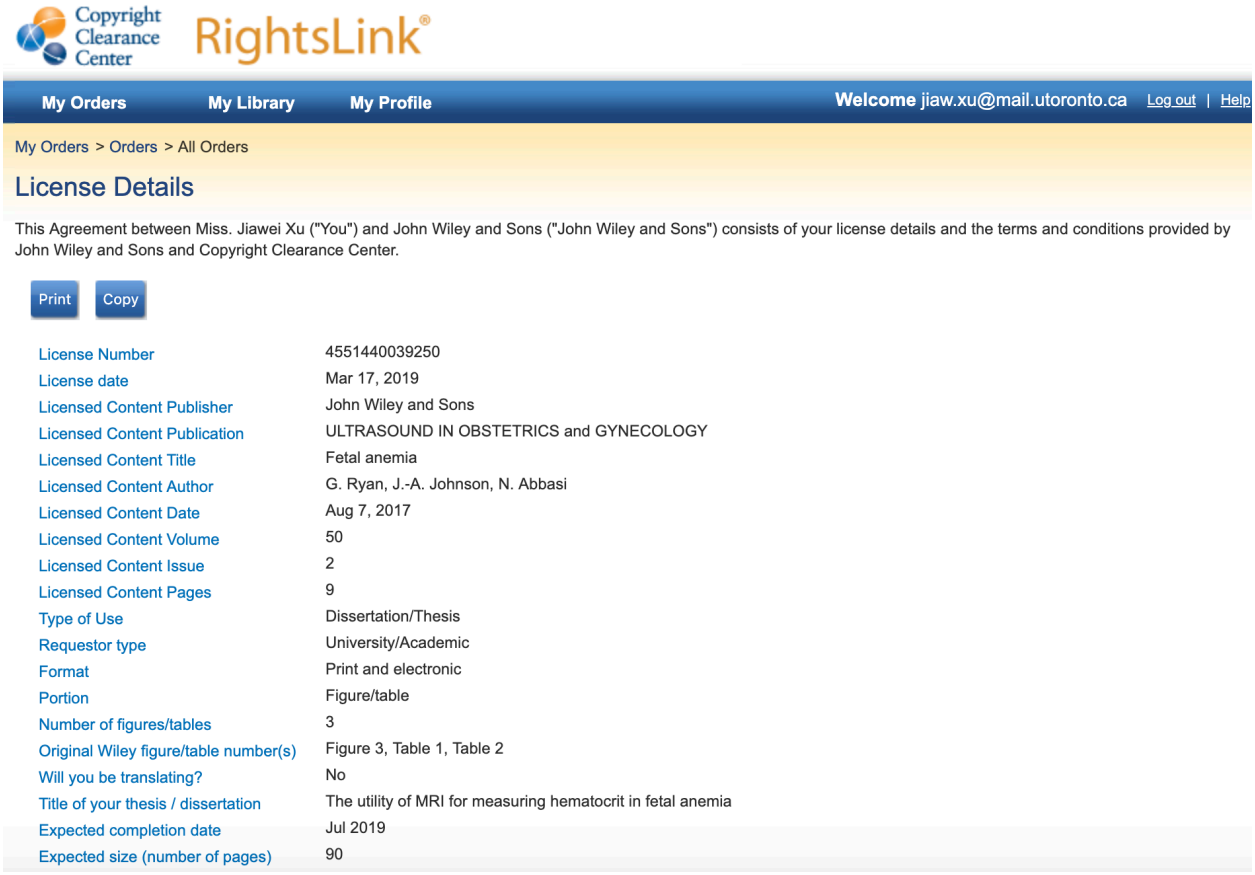

Copyright Clearance Center RightsLink®

My Orders | My Library | My Profile | Welcome jiaw.xu@mail.utoronto.ca | Log out | Help

My Orders > Orders > All Orders

License Details

This Agreement between Miss. Jiawei Xu ("You") and John Wiley and Sons ("John Wiley and Sons") consists of your license details and the terms and conditions provided by John Wiley and Sons and Copyright Clearance Center.

Print Copy

License Number	4551440039250
License date	Mar 17, 2019
Licensed Content Publisher	John Wiley and Sons
Licensed Content Publication	ULTRASOUND IN OBSTETRICS and GYNECOLOGY
Licensed Content Title	Fetal anemia
Licensed Content Author	G. Ryan, J.-A. Johnson, N. Abbasi
Licensed Content Date	Aug 7, 2017
Licensed Content Volume	50
Licensed Content Issue	2
Licensed Content Pages	9
Type of Use	Dissertation/Thesis
Requestor type	University/Academic
Format	Print and electronic
Portion	Figure/table
Number of figures/tables	3
Original Wiley figure/table number(s)	Figure 3, Table 1, Table 2
Will you be translating?	No
Title of your thesis / dissertation	The utility of MRI for measuring hematocrit in fetal anemia
Expected completion date	Jul 2019
Expected size (number of pages)	90

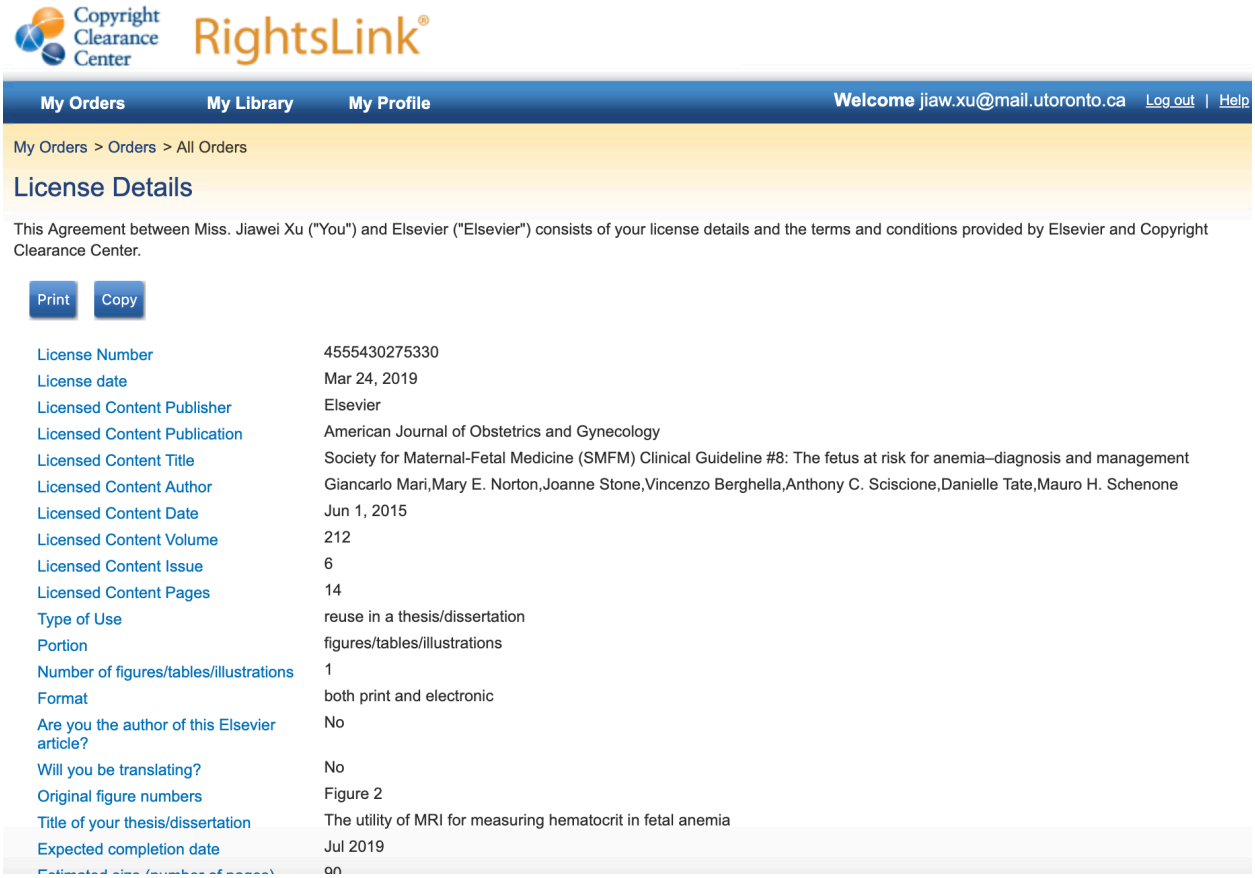

Copyright Clearance Center RightsLink®

My Orders | My Library | My Profile | Welcome jiaw.xu@mail.utoronto.ca | Log out | Help

My Orders > Orders > All Orders

License Details

This Agreement between Miss. Jiawei Xu ("You") and Elsevier ("Elsevier") consists of your license details and the terms and conditions provided by Elsevier and Copyright Clearance Center.

Print Copy

License Number	4555430275330
License date	Mar 24, 2019
Licensed Content Publisher	Elsevier
Licensed Content Publication	American Journal of Obstetrics and Gynecology
Licensed Content Title	Society for Maternal-Fetal Medicine (SMFM) Clinical Guideline #8: The fetus at risk for anemia–diagnosis and management
Licensed Content Author	Giancarlo Mari,Mary E. Norton,Joanne Stone,Vincenzo Berghella,Anthony C. Sciscione,Danielle Tate,Mauro H. Schenone
Licensed Content Date	Jun 1, 2015
Licensed Content Volume	212
Licensed Content Issue	6
Licensed Content Pages	14
Type of Use	reuse in a thesis/dissertation
Portion	figures/tables/illustrations
Number of figures/tables/illustrations	1
Format	both print and electronic
Are you the author of this Elsevier article?	No
Will you be translating?	No
Original figure numbers	Figure 2
Title of your thesis/dissertation	The utility of MRI for measuring hematocrit in fetal anemia
Expected completion date	Jul 2019
Estimated size (number of pages)	90

Permission is granted for the use of Fig 1, p.3 in the article detailed below in your PhD thesis only. Please include complete reference and copyright to Cold Spring Harbor Laboratory Press.

Best wishes for success with your thesis,

Carol C. Brown
Books Development, Marketing and Sales
Cold Spring Harbor Laboratory Press
500 Sunnyside Blvd
Woodbury, New York 11797
516 422 4038 ph.
516 422 4095 fx.
brown@cshl.edu

-----Original Message-----
From: reprint@cshl.edu [mailto:reprint@cshl.edu]
Sent: Tuesday, March 19, 2019 4:50 PM
To: Reprint
Subject: CSHL Press Reprint Permission Request Form

Default Intro
Default Intro - line2

Name: Jiawei Xu
CompanyInstitution: University of Toronto
Library Address:
Library Address (line 2):
City:
State (US and Canada):
Country:
Zip:
Title:
Lab/Department:
Phone:
Fax:
Email: jiaw.xu@mail.utoronto.ca
Title of Publication: The utility of MRI for measuring hematocrit in fetal anemia
Authors/Editors: Jiawei Xu
Date of Publication:
Publisher: University of Toronto
Title of CSHLP Journal/Book: old Spring Harbor Perspectives In Medicine,
Title of Article/Chapter: The Switch from Fetal to Adult Hemoglobin

License Details

This Agreement between Miss. Jiawei Xu ("You") and John Wiley and Sons ("John Wiley and Sons") consists of your license details and the terms and conditions provided by John Wiley and Sons and Copyright Clearance Center.

Print Copy

License Number	4573490409384
License date	Apr 21, 2019
Licensed Content Publisher	John Wiley and Sons
Licensed Content Publication	Magnetic Resonance in Medicine
Licensed Content Title	Relaxation properties of human umbilical cord blood at 1.5 Tesla
Licensed Content Author	Christopher K. Macgowan, John G. Sled, Mike Seed, et al
Licensed Content Date	Apr 5, 2016
Licensed Content Volume	77
Licensed Content Issue	4
Licensed Content Pages	13
Type of Use	Dissertation/Thesis
Requestor type	University/Academic
Format	Print and electronic
Portion	Figure/table
Number of figures/tables	3
Original Wiley figure/table number(s)	Figure 2, 4, 8
Will you be translating?	No
Title of your thesis / dissertation	The utility of MRI for measuring hematocrit in fetal anemia
Expected completion date	Jul 2019
Expected size (number of pages)	90

License Details

This Agreement between Miss. Jiawei Xu ("You") and John Wiley and Sons ("John Wiley and Sons") consists of your license details and the terms and conditions provided by John Wiley and Sons and Copyright Clearance Center.

Print Copy

License Number	4574450976422
License date	Apr 22, 2019
Licensed Content Publisher	John Wiley and Sons
Licensed Content Publication	Magnetic Resonance in Medicine
Licensed Content Title	Non-invasive evaluation of blood oxygen saturation and hematocrit from T1 and T2 relaxation times: In-vitro validation in fetal blood
Licensed Content Author	Sharon Portnoy, Mike Seed, John G. Sled, et al
Licensed Content Date	Feb 12, 2017
Licensed Content Volume	78
Licensed Content Issue	6
Licensed Content Pages	8
Type of Use	Dissertation/Thesis
Requestor type	University/Academic
Format	Print and electronic
Portion	Figure/table
Number of figures/tables	1
Original Wiley figure/table number(s)	Figure 1
Will you be translating?	No
Title of your thesis / dissertation	The utility of MRI for measuring hematocrit in fetal anemia
Expected completion date	Jul 2019
Expected size (number of pages)	90

Sharon Portnoy | Jiawei Xu 11:41 AM

Re: Permission request

Hi Jiawei,

Please feel free to include Figures 5.9 and 5.13 (with appropriate citation) in your Master's thesis.

Best of luck,
Sharon

From: Jiawei Xu <amy.xu@sickkids.ca>
Sent: July 24, 2019 11:38:41 AM
To: Sharon Portnoy <sharon.portnoy@sickkids.ca>
Subject: Permission request

Hi Sharon,

I am completing my Master's thesis entitled "The utility of MRI for estimating hematocrit in fetal anemia".

My thesis will be available in full text on the internet for reference, study and / or copy. Except in situations where a thesis is under embargo or restriction, the electronic version will be accessible through the U of T Libraries web pages, the Library's web catalogue, and also through web search engines. I will also be granting Library and Archives Canada and ProQuest/UMI a non-exclusive license to reproduce, loan, distribute, or sell single copies of my thesis by any means and in any form or format. These rights will in no way restrict re-publication of the material in any other form by you or by others authorized by you.

I would like permission to allow inclusion of the following material in my thesis: **Figure 5.9 on page 86 and Figure 5.13 on page 90 from your thesis entitled "Fetal Magnetic Resonance Oximetry", 2018 (http://hdl.handle.net/1807/91949).** The material will be attributed through a citation.

Please confirm in writing or by email that these arrangements meet with your approval.

Sincerely

Jiawei (Amy) Xu

License Details

This Agreement between Miss. Jiawei Xu ("You") and John Wiley and Sons ("John Wiley and Sons") consists of your license details and the terms and conditions provided by John Wiley and Sons and Copyright Clearance Center.

License Number	4574591048202
License date	Apr 23, 2019
Licensed Content Publisher	John Wiley and Sons
Licensed Content Publication	Transfusion
Licensed Content Title	Should optimal timing between two intrauterine transfusions be based on estimated daily decrease of hemoglobin or on measurement of fetal middle cerebral artery peak systolic velocity?
Licensed Content Author	Louise Ghesquière, Véronique Houfflin-Debarge, Hélène Behal, et al
Licensed Content Date	Mar 14, 2017
Licensed Content Volume	57
Licensed Content Issue	4
Licensed Content Pages	6
Type of Use	Dissertation/Thesis
Requestor type	University/Academic
Format	Print and electronic
Portion	Figure/table
Number of figures/tables	1
Original Wiley figure/table number(s)	Table 1
Will you be translating?	No
Title of your thesis / dissertation	The utility of MRI for measuring hematocrit in fetal anemia
Expected completion date	Jul 2019
Expected size (number of pages)	90